Particle Sources

Luca Serafini *INFN-Milan and University of Milan*

- **Ion Sources (*plasma physics of gas discharge, potential distribution, ionisation processes, magnetic confinement*)**

- **Electron Sources (*Thermoionic emission vs. Laser driven Photocathodes*)**

Emphasys on Beam Physics rather than on Plasma / Solid State Physics

- **Particle Beam Generation and Acceleration (first stage):**

  Space Charge diode saturation in CW / Long Pulse:

  Child-Langmuir Law ***(limitation in beam current density)***

  Beyond Child-Langmuir: emission in short transients

  RF Photo-Injectors ***for High Brightness Beams (X-ray FEL)***

Ion Sources: plasma physics of ion production

Ion generation inside the plasma via gas discharge

Plasma confinement sets up equilibrium

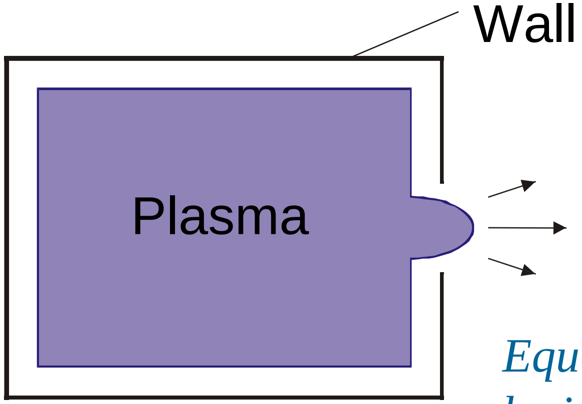

Equilibrium is locally broken by ion extraction from plasma

- **Plasma** : a hot gas containing free electrons, ions and neutral atoms.
- **Quasineutrality** : plasma (macroscopically) quasineutral if the number of positive charges per unit volume equals the negative charge density (electric field of single charges is screened over distances larger than the Debye length, usually microscopic)

$$\lambda_d = \sqrt{\frac{k_B T_e \varepsilon_o}{e^2 n_i}}$$

Ion Sources: plasma physics of ion production

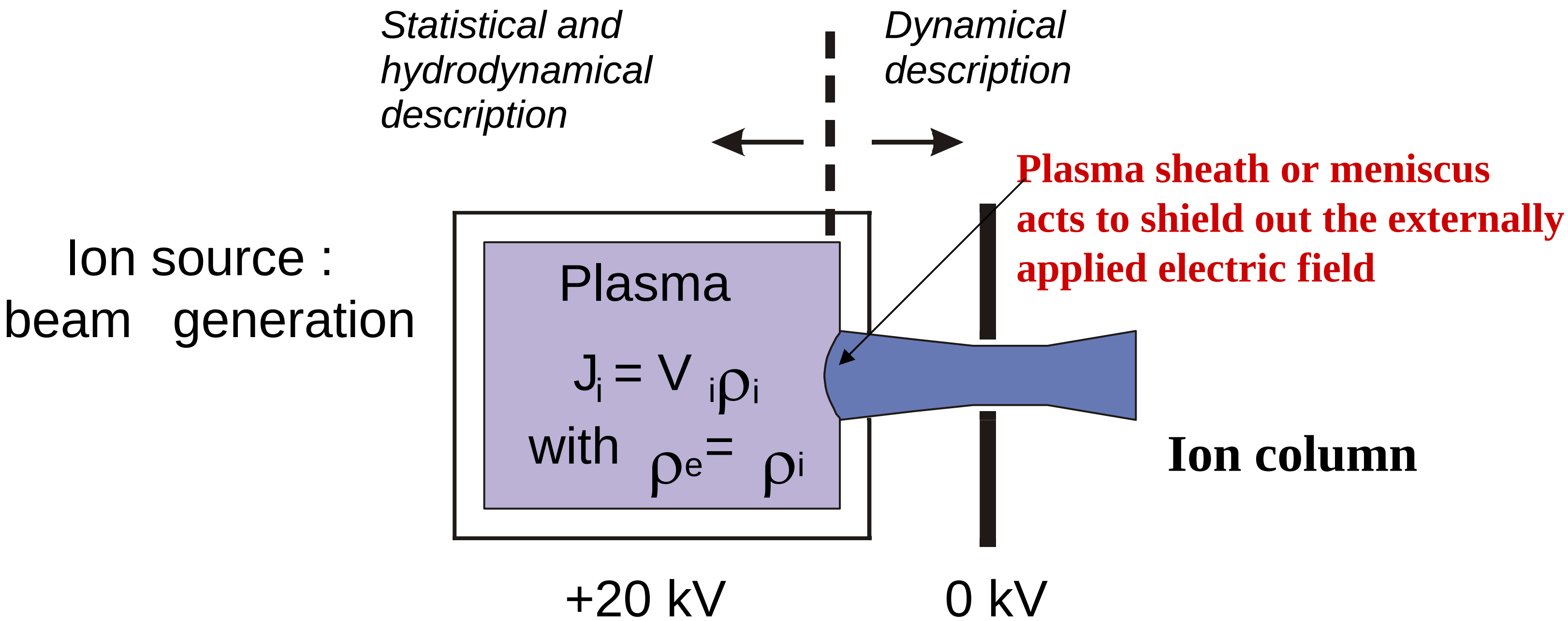

- The ion current is determined only by ion temperature, ion density and area of extraction opening

Ion Sources: plasma physics of ion production

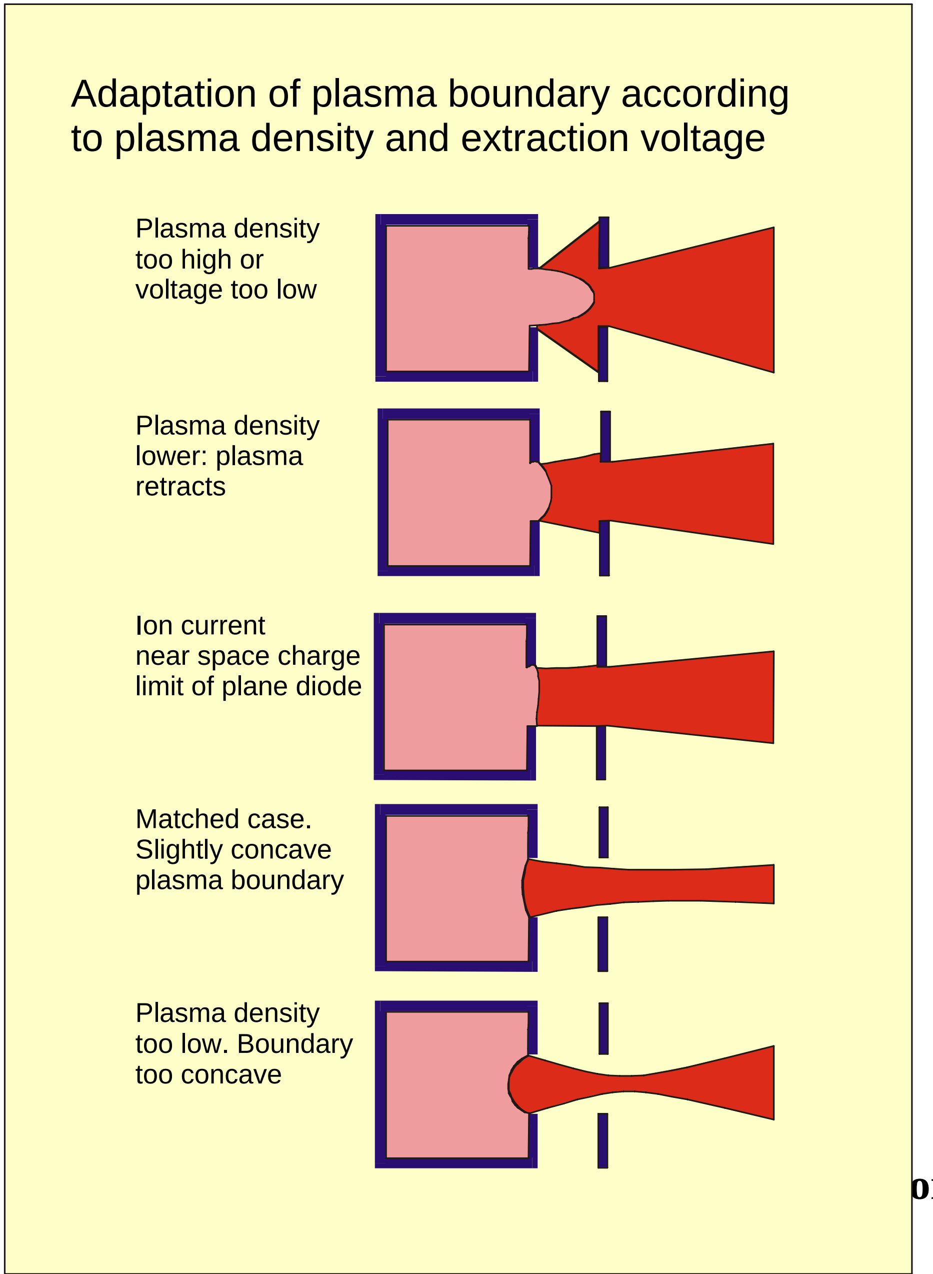

Ion Sources: plasma physics of ion production

- ***Collisional processes between plasma particles (inelastic collisions) bring to ionization***

Electron impact ionization

Simple case : $e^- + He \rightarrow He^+ + 2e^-$ with binding energy above 25 eV

then $e^- + He^+ \rightarrow He^{2+} + 3e^-$ with binding energy above 50 eV

More complex : including ionisation of molecule, e/atoms, ion/atoms, ions/molecule … collisions :

$e^- + H_2 \rightarrow H^0 + H^+ + 2e^-$

$e^- + H_2 \rightarrow H^+ + H^+ + 3e^-$

$e^- + H_2 \rightarrow H_2^+ + 2e^-$

$e^- + H_2^+ \rightarrow H^0 + H^+ + e^-$

Table 2 Typical ionisation potential ranges :

Ion Ionisation	Potential (eV)
Oxygen 5+ to 6+	138.1
Oxygen 0+ to 6+	433.1
Oxygen 7+ to 8+	871
Lead 26+ to 27+	874
Lead 0+ to 27+	9200
Lead 81+ to 82+	91400

Ion Sources: magnetic confinement necessary to improve ionization

- The maximum charge state that can be attained is limited by the maximum incident electron energy.

- *Multi-step ionisation is thus the only really feasible route to high-charge-state ions but this process takes time.*

- This time depends on plasma density and ionisation cross section - must be shorter than ion lifetime in the plasma.

Confining electrons and ions by means of a magnetic field improves this process

Ion Sources: magnetic confinement to improve ionization -> magnetic mirror effect

axial confinement due to conservation of magnetic momentum M and total energy E_{tot}

$$M = \frac{mv_{\perp}^2}{2B} = \frac{mv_{\perp\,\min}^2}{2B_{\min}} \qquad E_{tot} = \frac{1}{2}mv_{\perp}^2 + \frac{1}{2}mv_{//}^2 + E_p$$

$$E_{tot} = \frac{1}{2}mv_{\perp\,\min}^2 + \frac{1}{2}mv_{//\,\min}^2 + E_p = MB_{\min} + \frac{1}{2}mv_{//\,\min}^2 + E_p$$

if $v_{//}(z_{max}) = 0$ we have : $$\frac{1}{2}mv_{//\,\min}^2 = \frac{1}{2}mv_{\perp}^2(z_{mac}) - MB_{\min}$$

so $$v_{//\min}^2 = v_{\perp\min}^2\left(\frac{B_{\max}}{B_{\min}} - 1\right) \qquad \alpha \equiv \frac{v_{\perp\min}}{v_{//\min}} \geq \sqrt{\frac{B_{\max}}{B_{\min}} - 1}$$

trapping condition

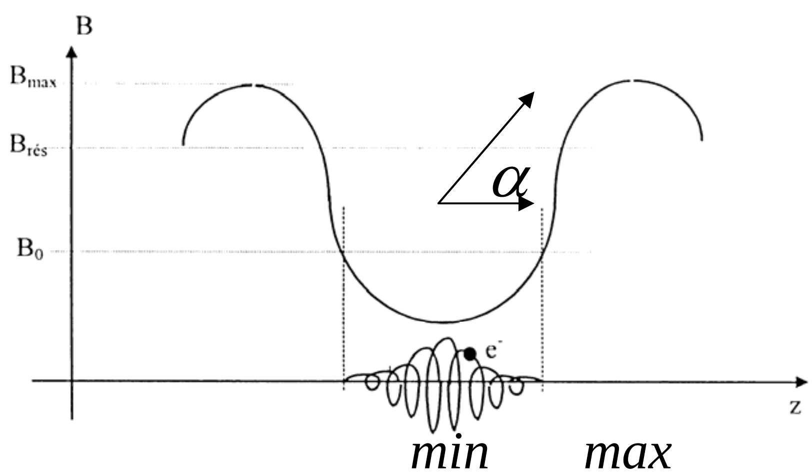

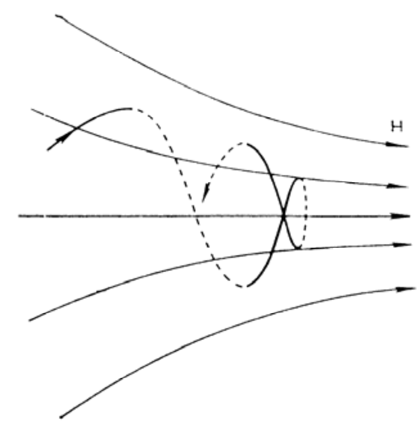

Simplest example: the Penning ion source

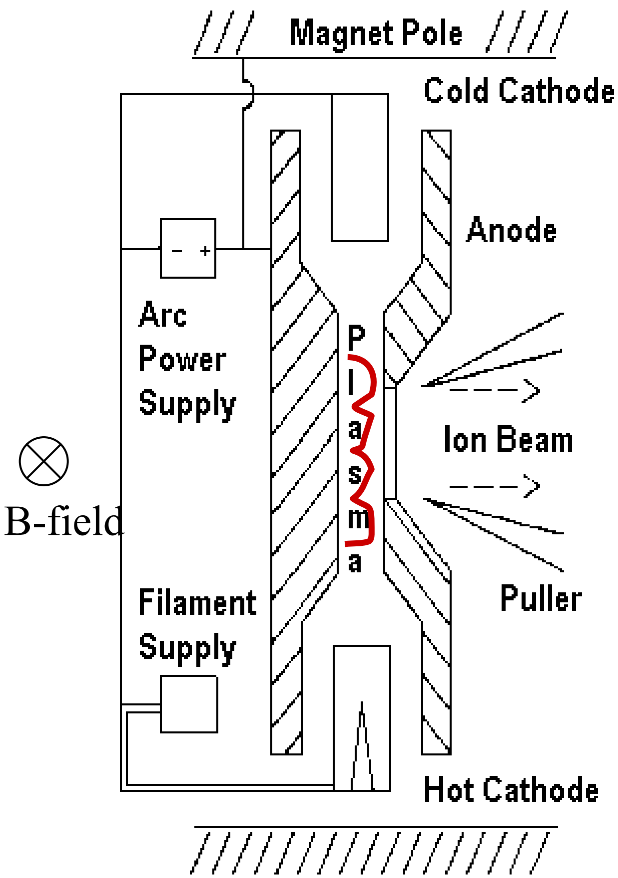

Electrons are emitted by the cathode , usually by thermoionic emission, and accelereted to an anode. Some of these **primary electrons** have collisions with gas atoms and ionize them. **Secondary electrons** from these collisions can be accelerated toward the anode to energies depending on the potential distribution and the starting point of the electron.

If a **ring or cylindrical anode is immersed in an axial magnetic field** with an electron emitter perpendicular to that field, electrons in the discharge plasma are forced into **cycloidal paths** thus increasing their path to the walls and **increasing, thereby, the probability of an ionising collision** with the neutrals.

electron trajectories

More efficient scheme for high current protons: the Duo-plasmatron

Anode Double Layer
As an ion source

Potential distribution

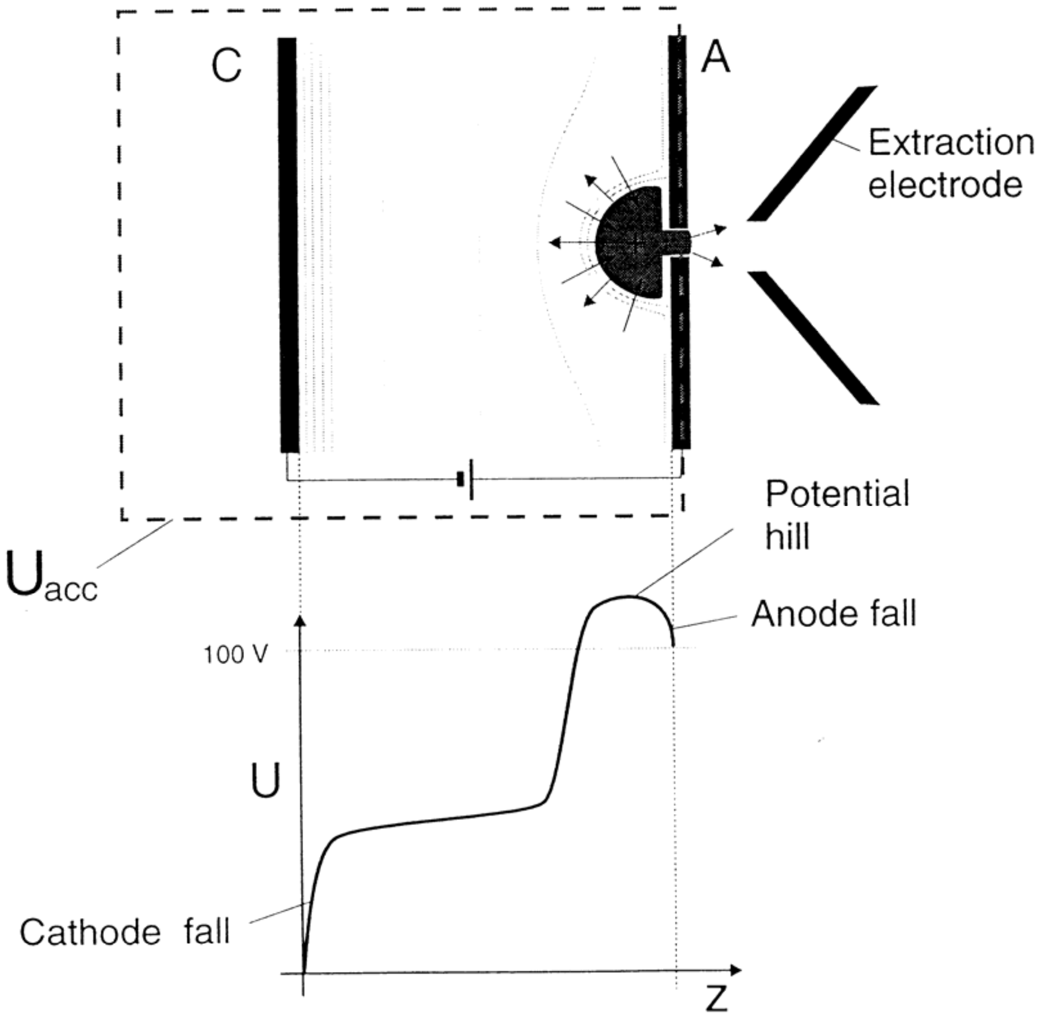

Duo-plasmatron

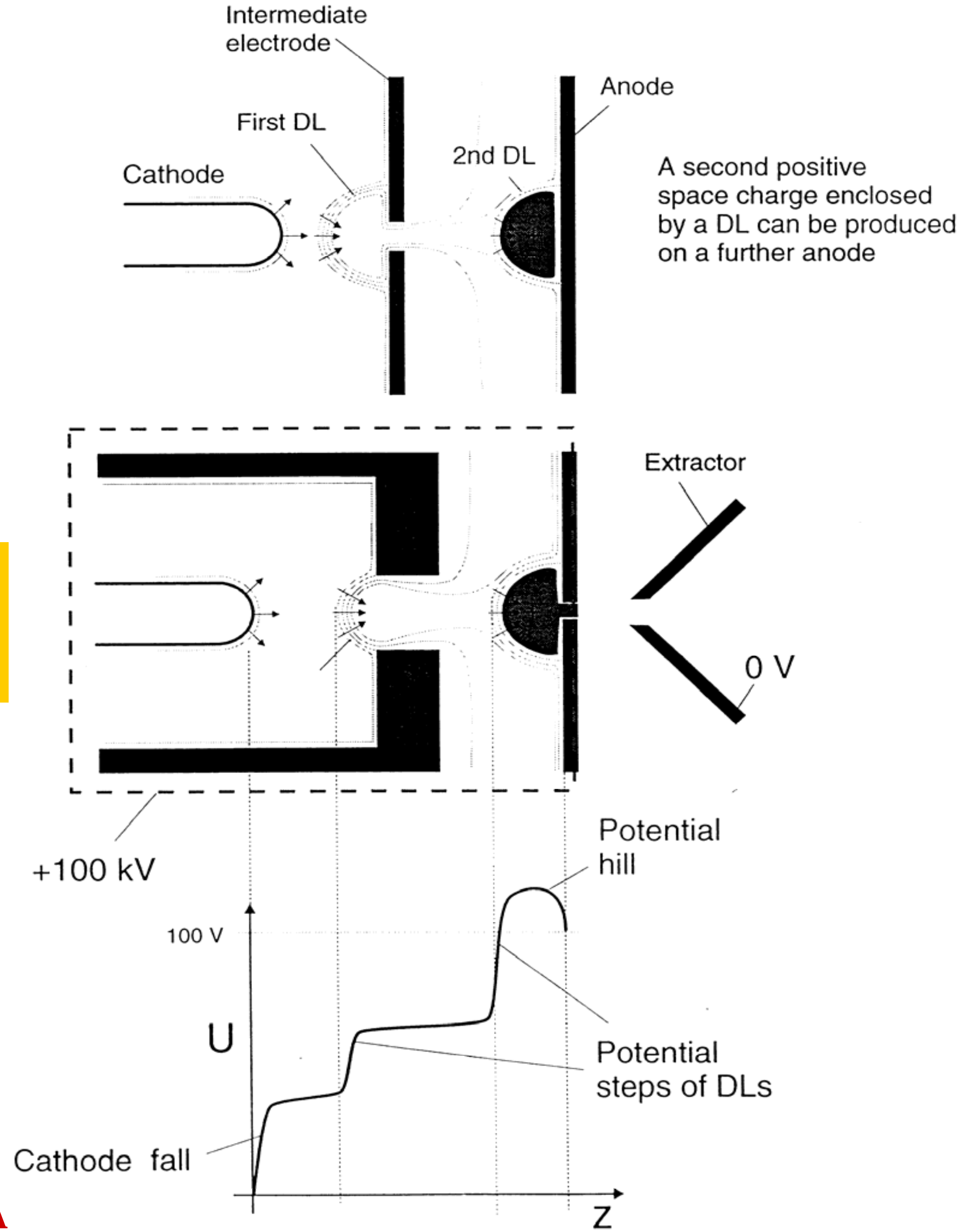

M.v. Ardenne 1955

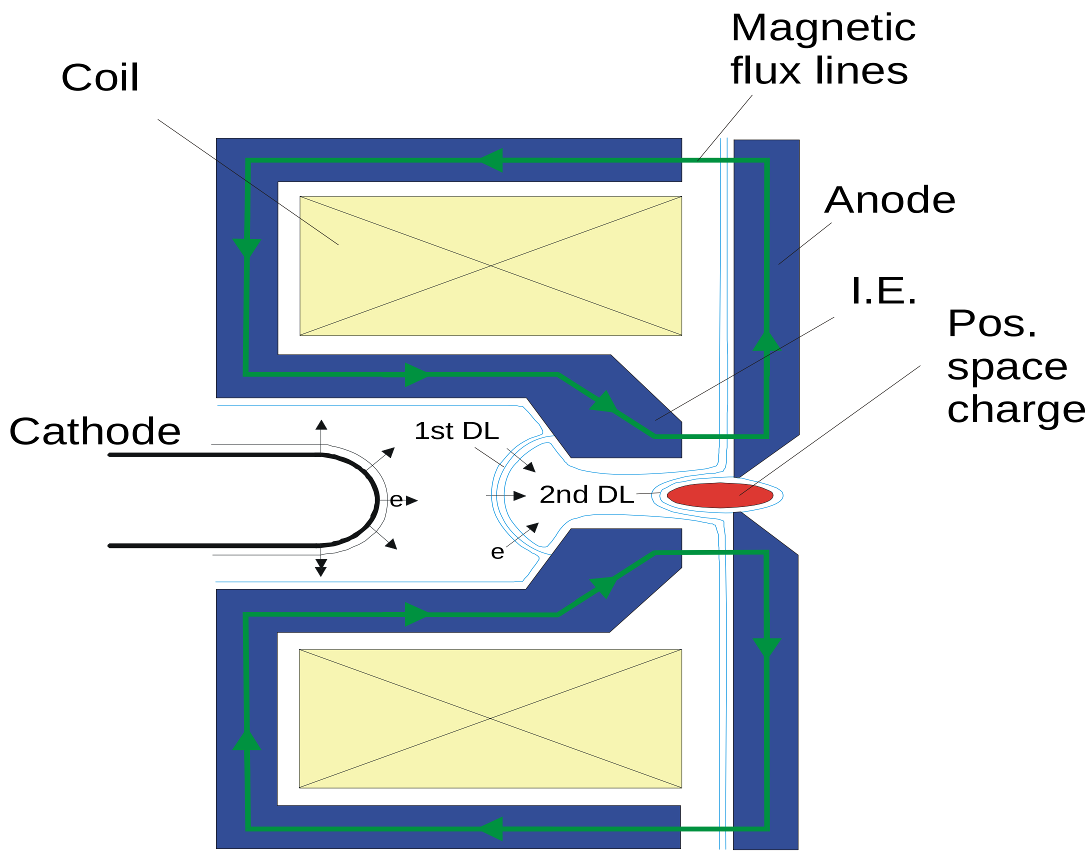

Duo-plasmatron for protons

limited to single charge state ions

- "duo"= two times plasma compression i.e. by DLs and mag. field
- Advantages: Simple, robust, cheap high currents, any gas
- Still used at CERN as "workhorse" (300 mA protons)

Beam Formation: Space Charge, Diode Saturation, Child-Langmuir Law

Gap variation to match boundary to given voltage

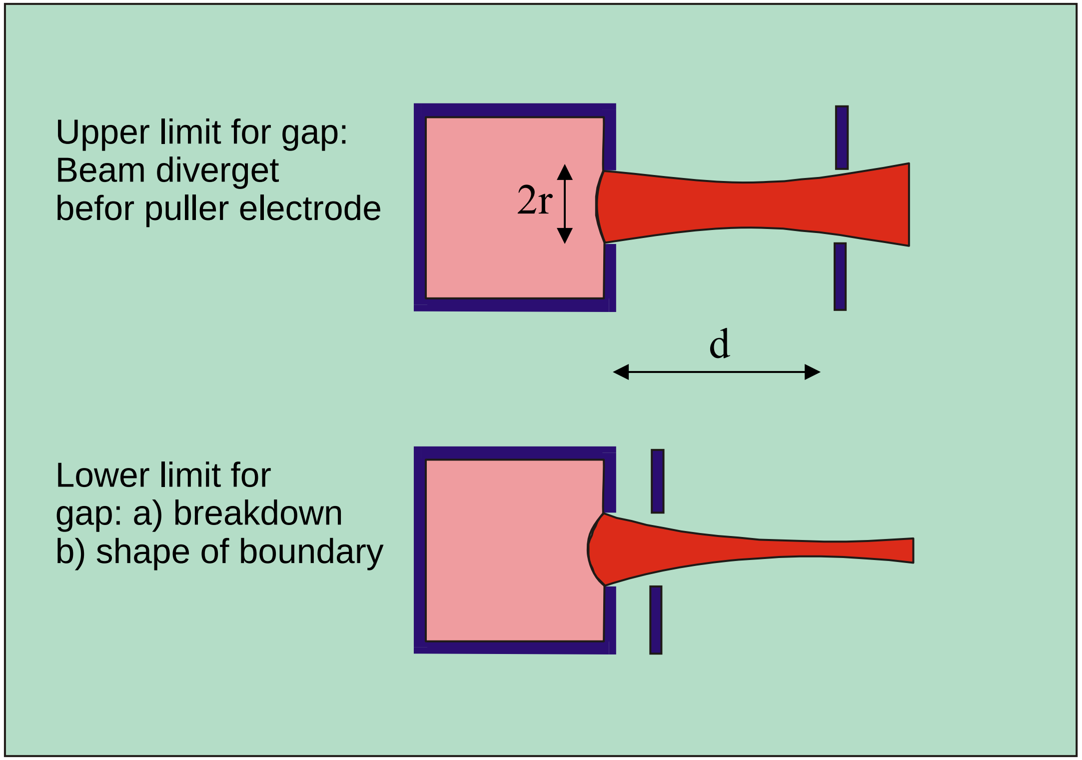

Ratio S = r/d must stay in a certain range
Best: S = 0.5 , Possible: 0.3......0.6

Ion current is restricted to a certain range for a given beam energy

Child-Langmuir Law

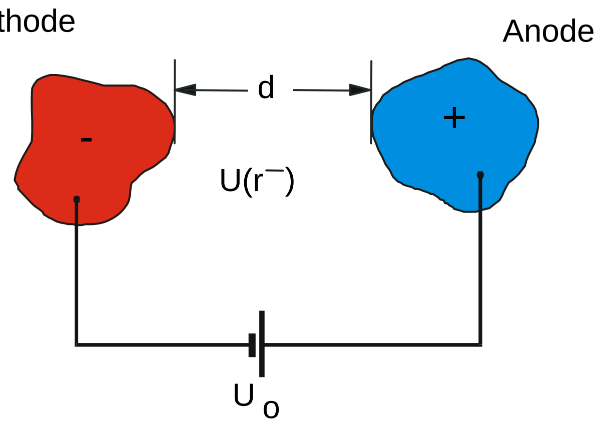

General case:

Assumptions:

a) Cathode can emitt infinite number of electrons

b) The electric field at the cathode is zero

c) Electrons are emitted with no initial velocity v = 0

$$\frac{d^2\phi}{dx^2} = -\frac{\rho}{\varepsilon_0}$$ Poisson's equation

$$J_x = \rho\dot{x} = const$$ Continuity equation bring to: $$\frac{d^2\phi}{dx^2} = -\frac{J}{\varepsilon_0\sqrt{2e/m}}\frac{1}{\sqrt{\phi}}$$

$$\frac{1}{2}m\dot{x}^2 = e\phi(x)$$ Equation of motion

Child-Langmuir Law for planar diode

A 1st integration of $$\frac{d^2\phi}{dx^2} = -\frac{J}{\varepsilon_0\sqrt{2e/m}}\frac{1}{\sqrt{\phi}}$$

gives $$\left(\frac{d\phi}{dx}\right)^2 = -\frac{4J}{\varepsilon_0\sqrt{2e/m}}\sqrt{\phi} + C$$

A 2nd integration: $$\phi(x) = U_0\left(\frac{x}{d}\right)^{4/3}$$

Substituting back for *J* : $$J = \frac{4}{9}\varepsilon_0\sqrt{\frac{2e}{m}}\frac{U_0{}^{3/2}}{d^2}$$

J independent on x

electrons $$J = 2.3\cdot 10^{-6}\frac{U_0{}^{3/2}}{d^2}$$

protons $$J = 5.4\cdot 10^{-8}\frac{U_0{}^{3/2}}{d^2}$$

100 kV over d=1 cm electrons J=73 A/cm^2 protons J=1.7 A/cm^2

Child-Langmuir Law for real diodes

The ion source current in a "diode" system is space charge limited

$I = P\,U^{3/2}$ $\qquad J = P\dfrac{U_0^{3/2}}{d^2}$

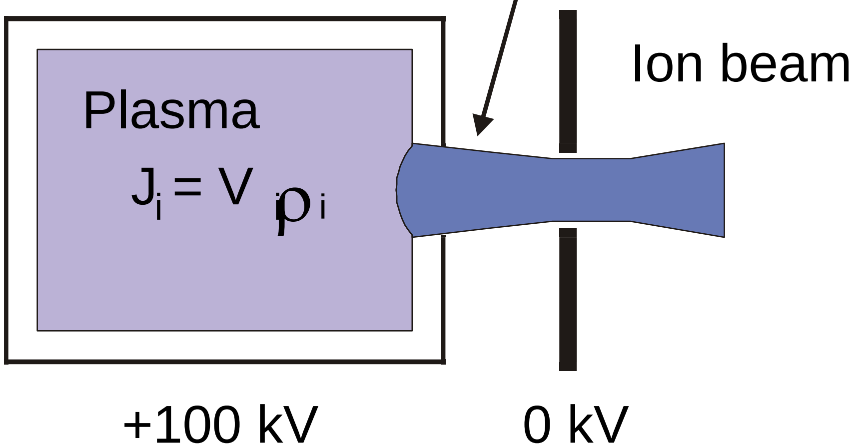

The ***Perveance P*** is a function of the geometry of electrodes, always smaller than ideal planar diode value

ideal $P_{el} = 2.3\ 10^{-6}$ *ideal* $P_{prot} = 5.4\ 10^{-8}$

max-$P_{el} = 7\ 10^{-7}$ *max-*$P_{prot} = 1.6\ 10^{-8}$

Three Generations of Electron Sources

- **Thermo-Ionic** **time-scale** Q_{bunch}=1-100 nC

  $B_n=10^{10}$ A/(m·rad)^2 **μs ⇒ ns** (ps with RF bunchers) I=0.1 ⇒ 10 A DC Diode (triode) with thermoionic cathode E ≈10 MV/m

- **Photo-Injectors** **time-scale** Q_{bunch}=0.1-10 nC

  $B_n=10^{15}$ A/(m·rad)^2 **ps** I=10 ⇒ 100 A RF Cavity with photo-cathode E ≈50-150 MV/m

- **Plasma Guns** **time-scale** Q_{bunch}=1-10 pC

  B_n =10^{14}-10^{15} A/(m·rad)^2 **fs** I≈ 1 kA

  Langmuir waves in cold plasmas +
  local wave-breaking E ≈ 1-10 GV/m

Transverse Brightness of Electron Beams

$$B_n = \frac{2I}{\varepsilon_{nx}\varepsilon_{ny}} \quad \left\lfloor \frac{A}{m^2 rad^2} \right\rfloor$$

I = peak current
ε_{nx} = rms normalized transverse emittance

Quality Factor : beam peak current density normalized to the rms beam divergence angle (linked to transverse **beam coherence**)

Round Beam : $\varepsilon_{nx} = \varepsilon_{ny} \quad , \quad J = I/\sigma^2 \quad \Rightarrow \quad B_n = \frac{2J}{(\sigma'\gamma)^2} = \frac{2J\sigma^2}{\varepsilon_n^2}$

$$\sigma = \sqrt{\varepsilon_n \beta/\gamma}$$

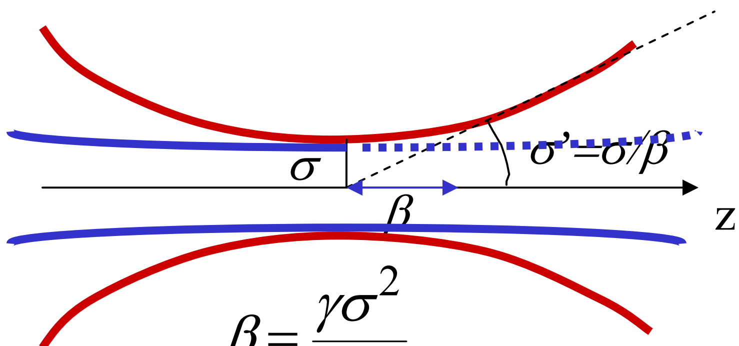

$$\beta = \frac{\gamma\sigma^2}{\varepsilon_n}$$

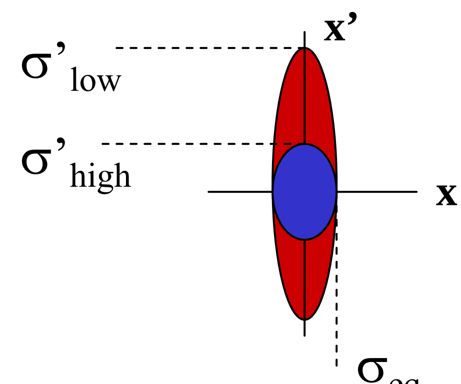

Brightness is crucial for many Applications

$$L_g \propto \frac{\gamma^{3/2}}{K\sqrt{B_n\left(1+K^2/2\right)}}$$

SASE FEL's

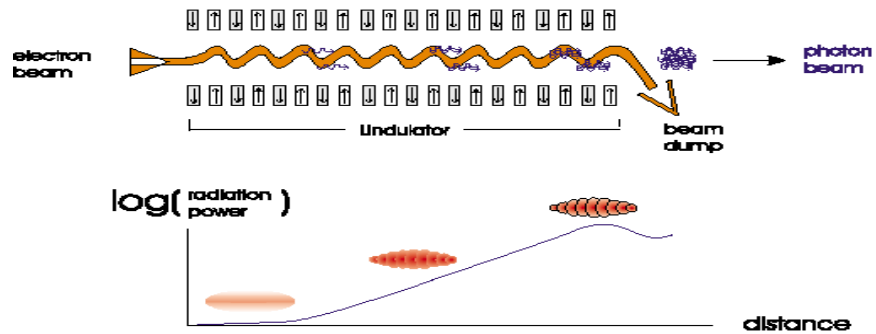

$$\varepsilon_n \le \sqrt{\gamma \frac{\Delta n_p}{n_p} \frac{\lambda_p}{2\pi}}$$

Plasma Accelerators

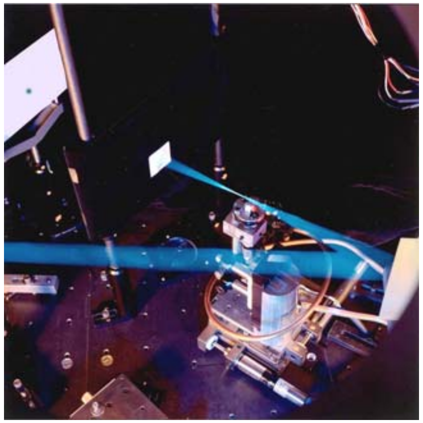

Courtesy of D. Umstadter, Univ. of Michigan

$$\Phi_p \approx 50 \quad \mu m$$

$$\lambda_p \approx 30 - 100 \quad \mu m$$

$$N_X \propto \Sigma_T f \frac{N_{e^-} N_{h\nu}}{\varepsilon_n \beta^*} \gamma \quad ; \quad \beta^* > \sigma_z$$

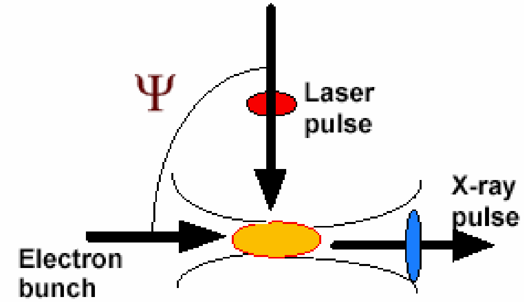

Fig. 2 Thomson scattering geometry

Relativistic Thomson Monochromatic X-Ray Sources

Thermoionic Injectors

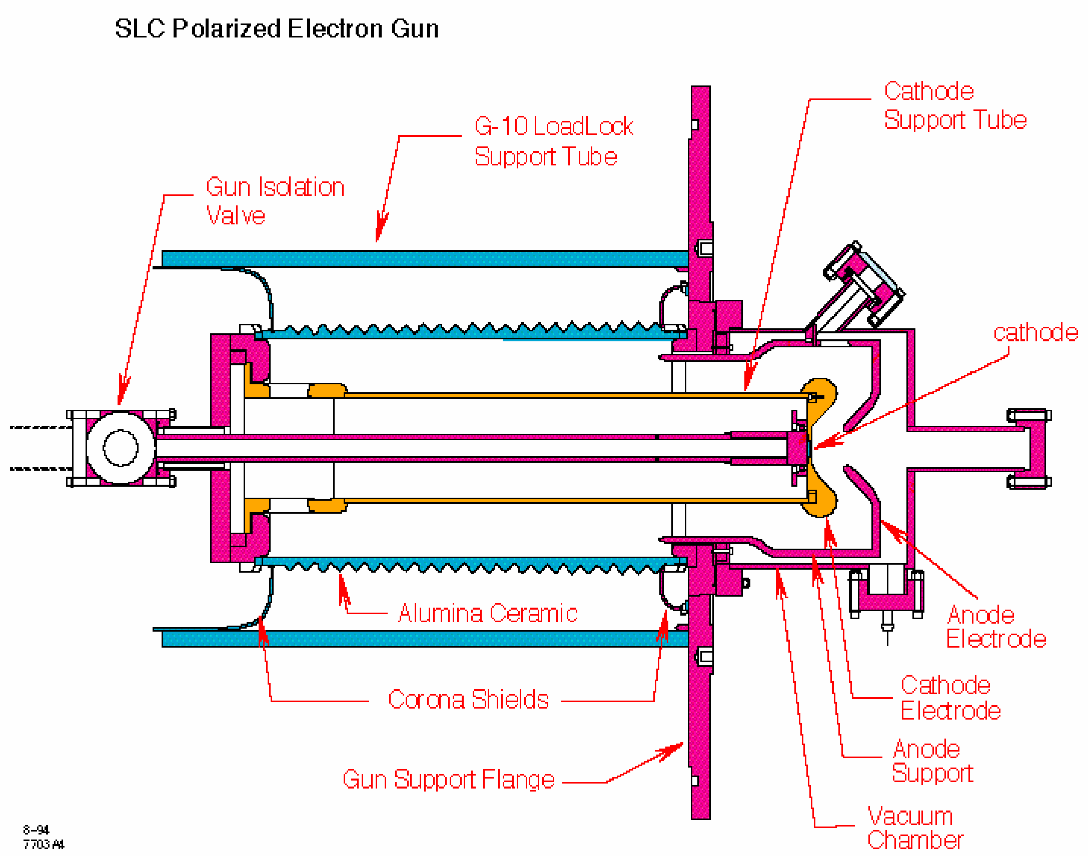

$$J_{\max}\left[A/cm^2\right] = 120T^2 e^{-W/k_B T}$$

$$W \equiv cathode\ \ work - function$$

$$T \equiv cathode\ \ temperature$$

LIMITATIONS

Cathode Emissivity $J < 20\ A/cm^2$

Diode Saturation

$\Downarrow$

Child-Langmuir Law $I = PV^{3/2}$

V=100 kV   I=15 A   with $P=5 \cdot 10^{-7}$

$\Downarrow$

Field limited

MATURE and CONSOLIDATED TECHNOLOGY

Radio-Frequency Photo-Injectors

Photo-Cathode Emissivity J < 10 kA/cm²
Prompt emission on a ps time scale

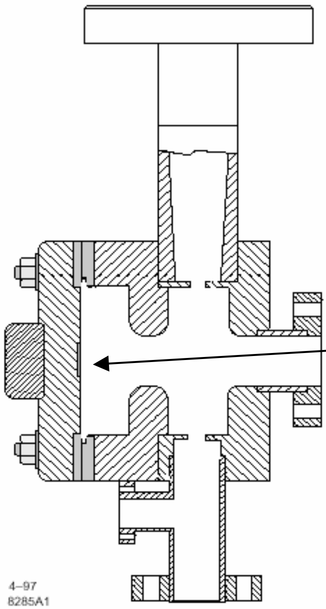

UCLA/SLAC/BNL
S-band next gen. RF Gun

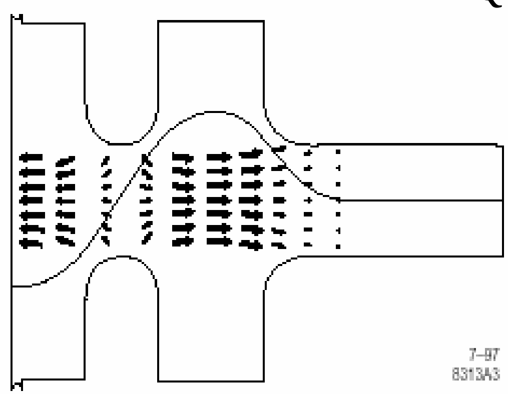

$$Q_{eff} = N_{electrons} / N_{laser-photons}$$

$$Q_{eff}\,(Cu \quad photo-cathode) \cong 5 \cdot 10^{-5}$$

$$W_{Cu} = 4.2eV, \; h\nu = 4.6eV$$

$$Q = 1 \;\; nC \;\; needs \;\; U_{las} = \frac{h\nu \cdot Q_{bunch}}{Q_{eff}} = 92 \;\; \mu J$$

LIMITATIONS

Transverse plasma oscillations
Time dependent space charge effects
dilution of projected emittance

Photocathode and/or laser disuniform.

PROBLEMS

Space and Time Jitters
Laser beam quality
Challenging Diagnostics (sub-ps)

Mature but non Consolidated Technology
Stability , repetibility , ease of tuning

All Optical Injectors (Plasma Guns)

CO.L.I.L.AC
Berkeley Lab

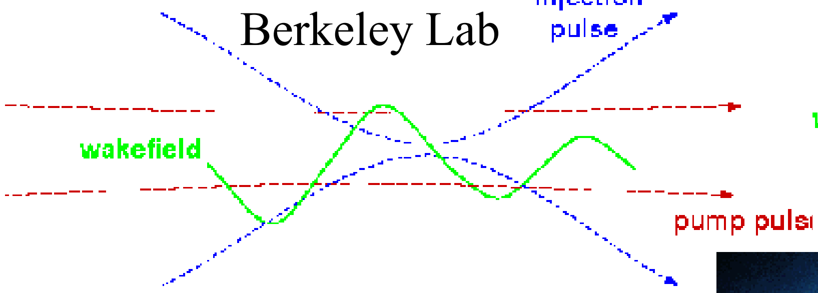

L.I.L.AC
Univ. of Michigan

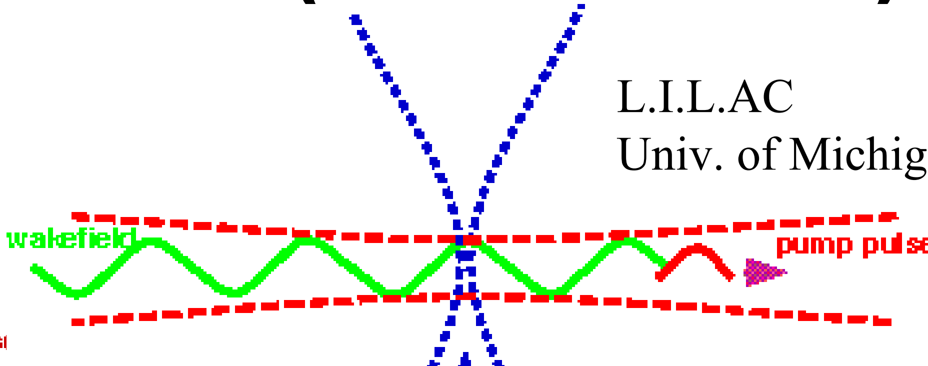

Tecnologia in fase Esplorativa
Solo risultati numerici sinora

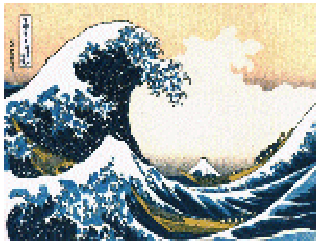

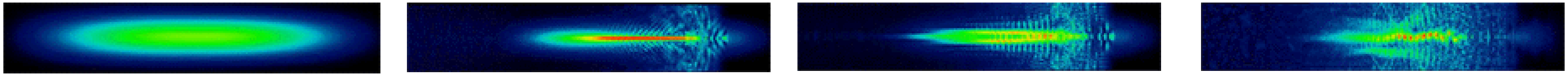

The Evolution of the Laser through a semi-infinite plasma slab (in 2D). The simulation box is moving at the speed of light towards the right.

1) @ 0.00mm - the plasma is at the right boundary of the simulation box. The initial laser pulse is Gaussian. **Plasma density: 10^{19} cm^{-3}**
2) @ 0.57mm- the simulation box is almost filled by the plasma. Relativistic Self-Focusing is effective. The fishbone structure is caused by bunching of the laser, and the separation is in plasma wavelength. (Laser wavelength is ten times smaller, i.e. 1 μm.)
3) @ 0.83mm - the laser pulse has evolved under relativistic filamentation sourced from self-focusing. Electric field is in excess of **100 GV/m**.
4) @ 1.82mm - after plasma wavebreaking the laser hose instability has grown to an incredible strength coupled to Raman scattering.

40 MeV electron were produced : Rutherford/UCLA/LLNL experiment for laser-plasma acceleration test

LIMITATIONS
plasma temperature (thermal emittance)

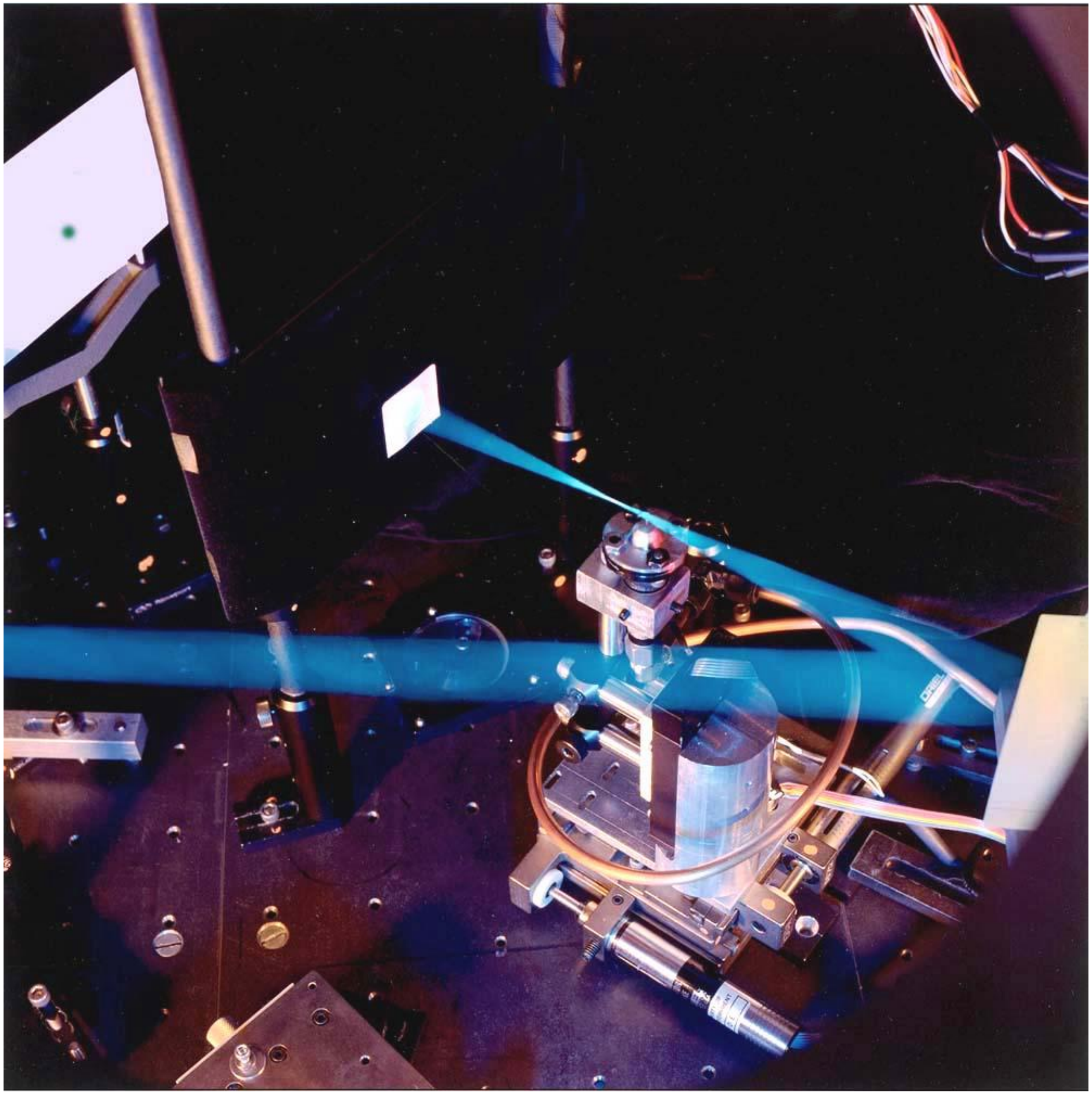

University of Michigan
D. Umstadter

Brief Review of
Beam Dinamycs in Photo-Injectors

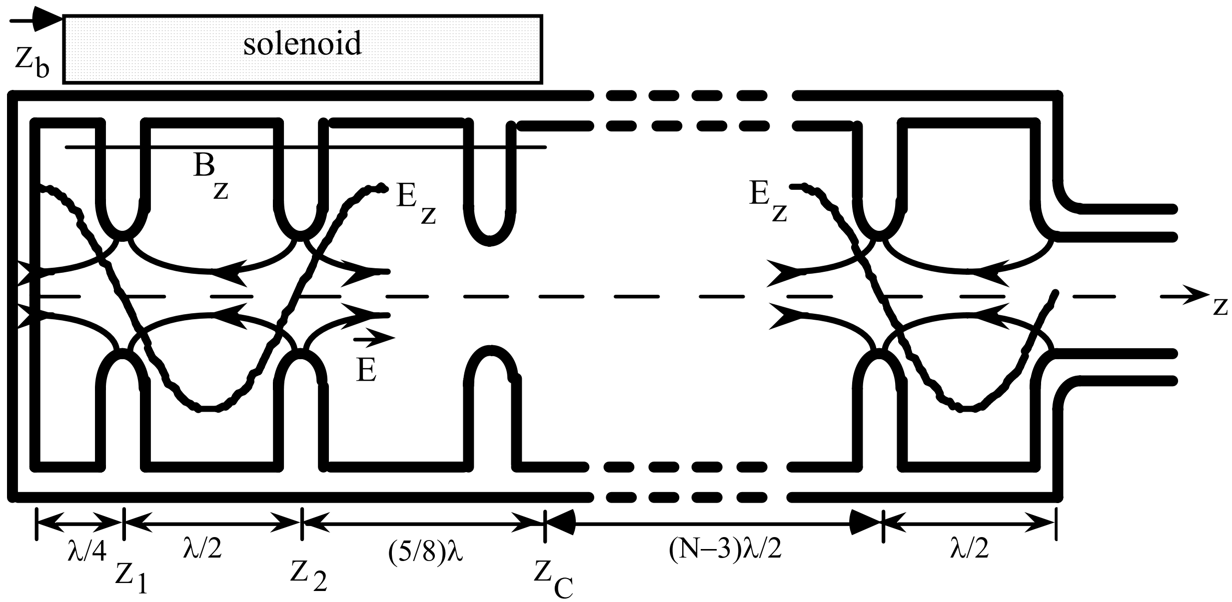

On-axis expansion of the $TM_{010\text{-}\pi}$ standing mode

E_0 = the peak field at the cathode
$k \equiv 2\pi/\lambda = \omega/c$
a_n = spatial harmonic coefficients functions of cavity geometry

$$\begin{cases} E_z = \mathcal{E}_z(r,z)\cdot\sin(\omega t+\varphi_0) \quad ; \quad \mathcal{E}_z(r,z) = E_0 \sum_{n=1,odd}^{\infty} a_n \cos(nkz) \\ E_r = \mathcal{E}_r(r,z)\cdot\sin(\omega t+\varphi_0) \quad ; \quad \mathcal{E}_r(r,z) = \frac{kr}{2} E_0 \sum_{n=1,odd}^{\infty} n\cdot a_n \sin(nkz) \quad ; \quad a_1 = 1 \\ \mathrm{B}_\theta = B_\theta(r,z)\cdot\cos(\omega t+\varphi_0) \quad ; \quad B_\theta(r,z) = c\,\frac{kr}{2}\mathcal{E}_z(r,z) \end{cases}$$

Beam Dinamycs in Photo-Injectors

Photo-electrons at photo-cathode surface are non relativistic (laser photon energy just overcomes cathode metal work-function)

$$T_{cat} = h\nu_{las} - W_S = 4.6 - 4.4 = 0.2 \;\; eV \;\; ; \;\; \beta_{cat} \cong 10^{-3} \;\; (\,for \;\; Cu \;\; cathodes)$$

Define dimensionless vector potential amplitude of RF field $\alpha \equiv \dfrac{eE_0}{2mc^2k}$

$$E_0 = 100 \;\; MV/m \;\; @ \;\; 2.856 \;\; GHz \Rightarrow \;\; \alpha = 1.6$$

Photo-electrons become relativistic in a distance much shorter than λ_{RF}

⇓

RF wave is able to capture electrons from rest if $\alpha > 1$

$$T = 1 \;\; MeV \;\; @ \;\; z = 1 \;\; cm \;\; (\,first \;\; cell \;\; length \;\; = \;\; 2.5 \;\; cm) \qquad \beta = 0.95$$

Beam Dinamycs in Photo-Injectors

Impulsive approximation
E_{RF} = DC field = E_{cat}

Equivalent relativistic motion with effective phase shift

$$E_{cat} \cong \mu E_0 \sin\varphi_0 \;\; ; \;\; \mu \equiv \sum_{n=1}^{\infty} a_n$$

$$z = ct - \frac{1}{2\mu\alpha k \sin\varphi_0}$$

$$\varphi = \varphi_0 - \frac{1}{2\mu\alpha \sin\varphi}$$

$$\gamma_2 = 1 + \frac{3\pi\alpha}{2}\sin\varphi + \alpha\cos\varphi$$

RF backward wave Component in half cell

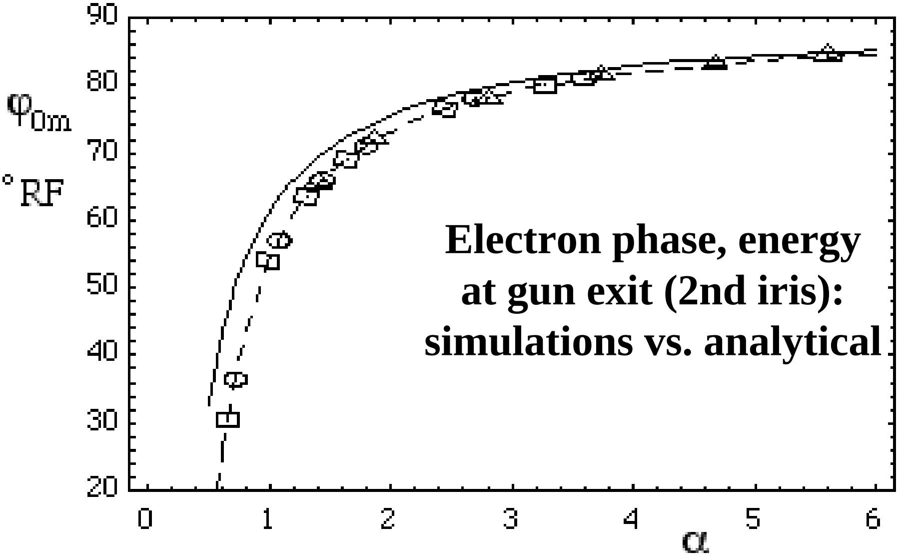

Electron phase, energy at gun exit (2nd iris): simulations vs. analytical

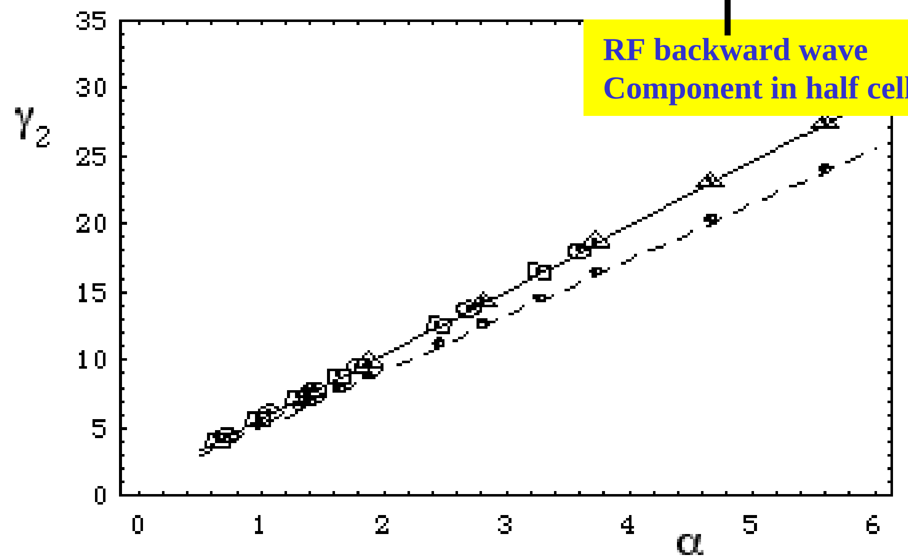

Beam Dinamycs in Photo-Injectors: overcome Child-Langmuir limitation

Laser driven RF Photo-Injectors work far from the (equivalent) diode saturation regime, well into the linear regime

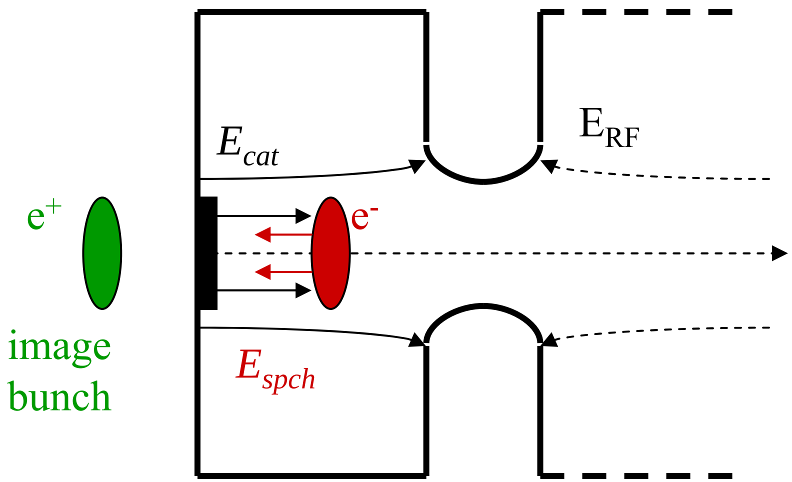

$$E_{spch} << E_{cat} \quad \Rightarrow \quad \frac{Q_{bunch}}{\pi \varepsilon_0 R^2} << E_{cat}$$

$$Q_{bunch}[nC] \;<<\; \frac{1}{25}\; E_{cat}[MV/m]\;(R[mm])^2$$

$$I \equiv \frac{Q_{bunch}}{\tau_{bunch}} \;\Rightarrow\; I \geq 100 \;\; A \;!!$$

$$Q_{bunch} \;<<\; 5.6 \;@\; (140 \;\; MV/m \;,\; 1 \;\; mm)$$

Beam Dinamycs in Photo-Injectors

themperature emittance @ photo-cathode (real liouvillian emittance)

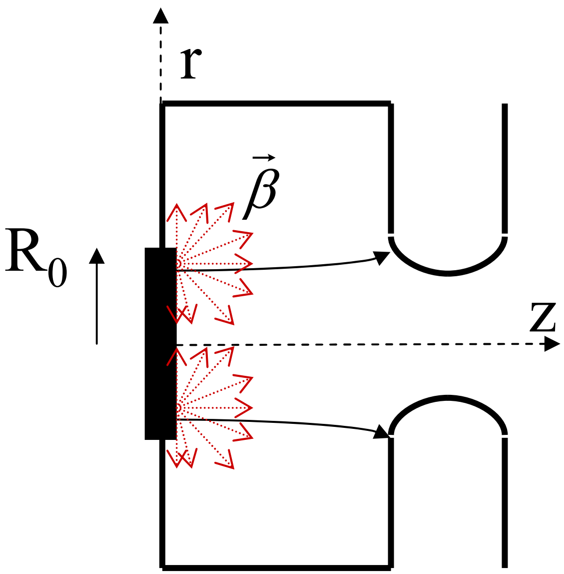

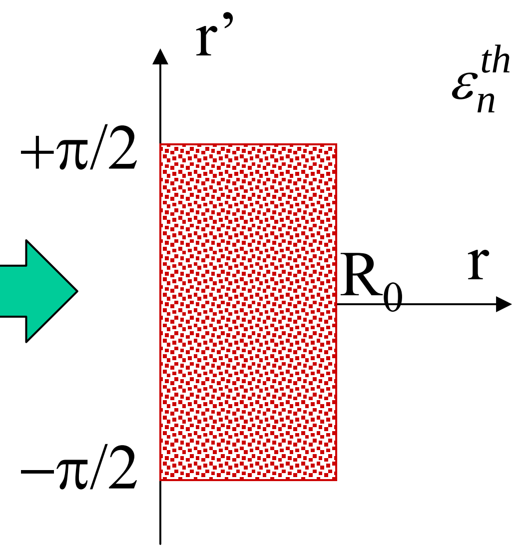

$$\varepsilon_n^{th} = \frac{\langle \beta\gamma \rangle}{2} \sqrt{\langle r^2 \rangle \langle r'^2 \rangle - \langle r r' \rangle^2}$$

$$\langle r^2 \rangle \equiv \frac{\int_0^{R_0} r^3 dr}{\int_0^{R_0} r dr}$$

$$\langle x^2 \rangle = \frac{\langle r^2 \rangle}{2}$$

$$\langle \beta\gamma \rangle \cong \langle \beta \rangle \cong \sqrt{2T_e / m_e c^2} = 2 \cdot 10^{-3} \sqrt{T_e[eV]} \quad \Rightarrow \quad \varepsilon_n^{th} = \frac{\pi \langle \beta \rangle R_0}{4\sqrt{6}}$$

$$\varepsilon_n^{th} \; [mm \cdot mrad] = 0.64 \;\; R_0[mm] \;\; \sqrt{T_e[eV]}$$

in absence of any channeling mechanism

Schematic View of the Envelope Equations (HOMDYN model)

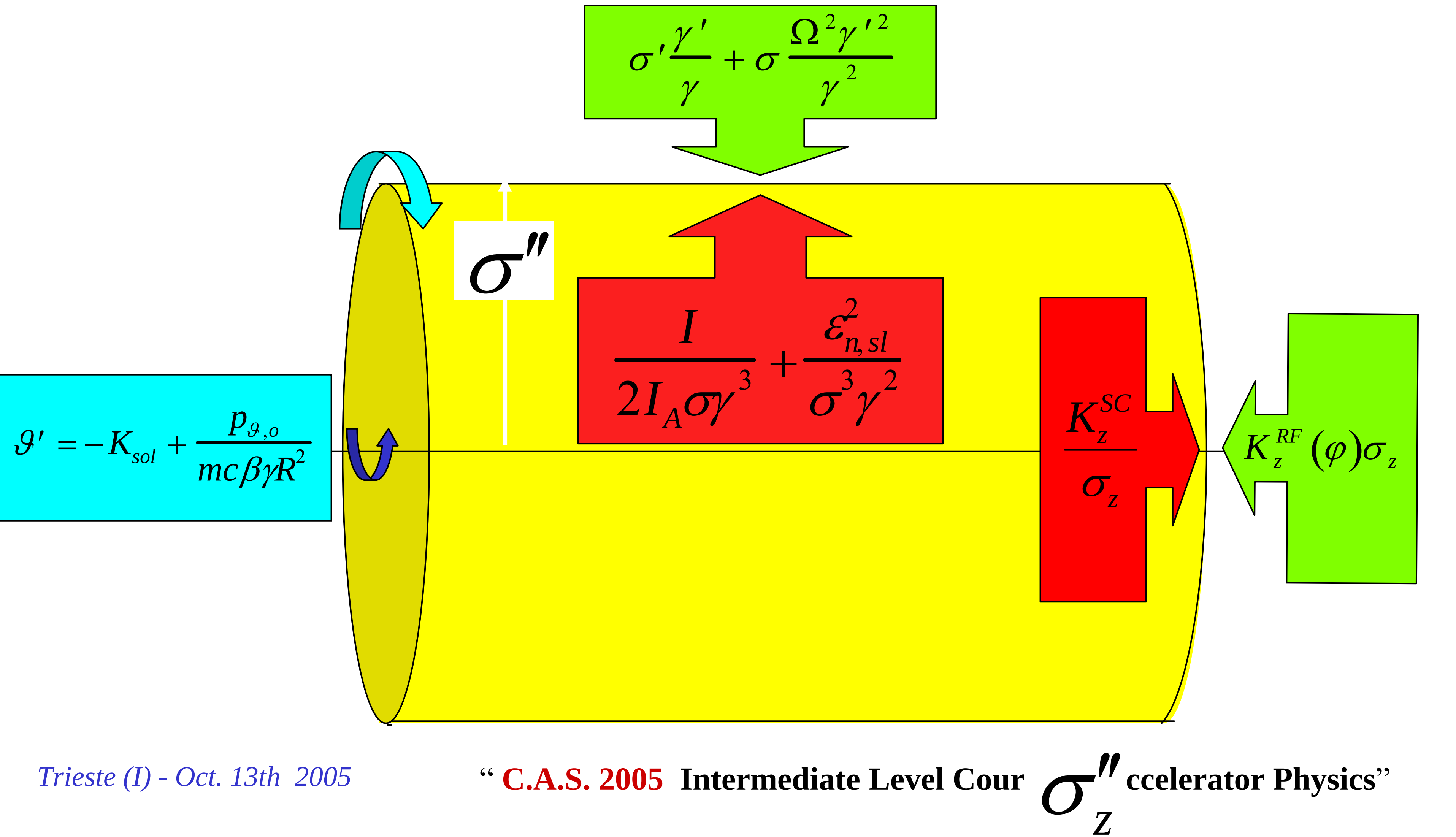

Cold Relativistic Plasma-Beams in Laminar Flow with time dependent Space Charge Fields

$$\frac{I}{I_A} = \frac{I}{17\ kA}$$

Plasma wavelength (sp. ch. oscillation) $\lambda_p = 2\pi \frac{\gamma}{\gamma'} = 2\pi L_{acc}$

Betatron wavelength $\lambda_\beta = 4\pi \frac{(I/I_A)}{\varepsilon_{th}\gamma'^2 \eta}$

γ' Accelerating gradient

$\eta \cong 1$ norm. amplit. of RF focusing

$L = \gamma_f / \gamma'$ Linac length

ε_{th} photocath. therm. emittance

At Linac exit

$$T = 1\ GeV\ ;\ \gamma_f = 2 \cdot 10^3\ ;\ \gamma' = 40\ m^{-1}\ \ I = 1\ kA\ ;\ \varepsilon_{th} = 5 \cdot 10^{-7}$$

$$\lambda_p / \lambda_\beta = 0.3$$

Betatron oscill. ~ 0.3
Plasma oscill. ~ 1
Synchrotron oscill. ~ 1/4

L.S., J.B. Rosenzweig, *PRE* 55 (1997) 7565

Brief Review of
Beam Dinamycs in Photo-Injectors

- The beam generated at the *photocathode surface* behaves like a **Single Component Relativistic Cold Plasma** all the way up to the injector exit (150 MeV, 1 GeV with compression)
- It is a *quasi-laminar* beam both in transverse (laminar flow) and longitudinal plane (lack of synchrotron motion)

$$\sigma'' + \sigma'\frac{\gamma'}{\gamma} + \sigma\frac{\Omega^2\gamma'^2}{\gamma^2} - \frac{I(\zeta)}{2I_A\sigma\gamma^3} \cancel{-\frac{\varepsilon_{n,sl}^2}{\sigma^3\gamma^2}} \approx 0$$

$$\gamma = \gamma_0 + \gamma' z \quad \gamma' \equiv \frac{E_{acc}}{mc^2} \quad \sigma' \equiv \frac{d\sigma}{dz} \qquad \Omega^2 = \left(\frac{eB_{sol}}{mc\gamma'}\right)^2 + \begin{Bmatrix} \approx 1/8 \ \ SW \\ \approx 0 \quad TW \end{Bmatrix}$$

$$\sigma \equiv \langle x^2 \rangle \quad slice \ \ \zeta = z - \beta ct$$

Normalized focusing gradient
(solenoid +RF foc.)

S.C.R.C.P. or Laminar Plasma-Beam

- Plasma launched at relativistic velocities along the propagation axis with equivalent ionization = $1/\gamma^2$; plasma confinement provided by external focusing (solenoids, ponderomotive RF focusing, acceleration)
- Spread in plasma frequency along the bunch $\Rightarrow$ strong time-dependent space charge effects $\Rightarrow$ inter-slice dynamics

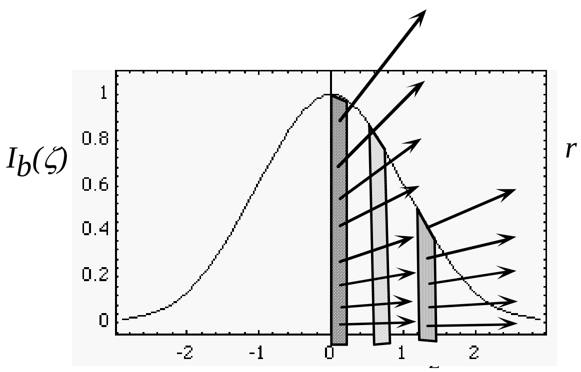

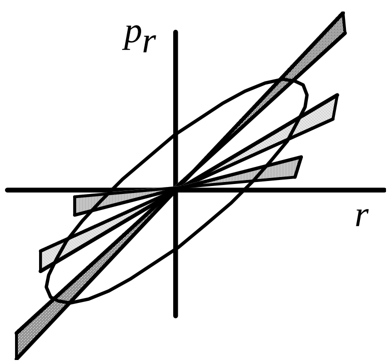

Per vedere questa immagine occorre QuickTime™ e un decompressore Animation.

Projected emittance (shadow) >> slice emittance (foil thickness)

© *M. Serafini*

$$\varepsilon_n \equiv \sqrt{\langle x^2\rangle\langle p_x^2\rangle - \langle xp_x\rangle^2} \quad >> \quad \varepsilon_{nsl} \equiv \sqrt{\langle x^2\rangle_\zeta\langle p_x^2\rangle_\zeta - \langle xp_x\rangle_\zeta^2}$$

Liouvillian emittance = foil volume

Emittance Compensation:

Controlled Damping of Plasma Oscillation

$$\gamma = \sqrt{\frac{8}{3}\frac{\hat{I}}{2I_o\varepsilon_{th}\gamma'}}$$

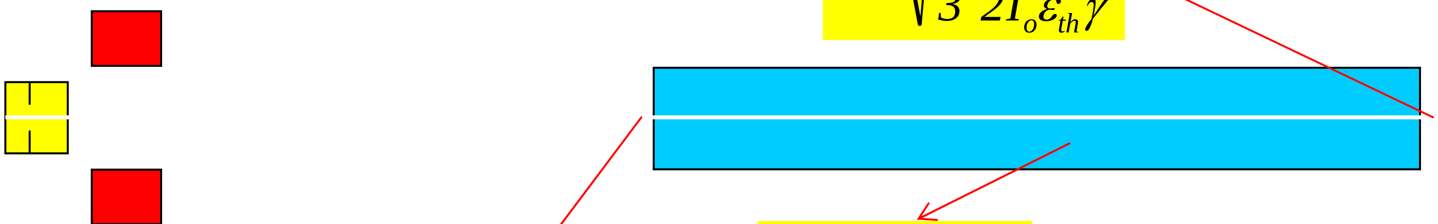

$$\sigma' = 0$$

$$\gamma' = \frac{2}{\sigma_w}\sqrt{\frac{\hat{I}}{3I_0\gamma}}$$

Brillouin Flow

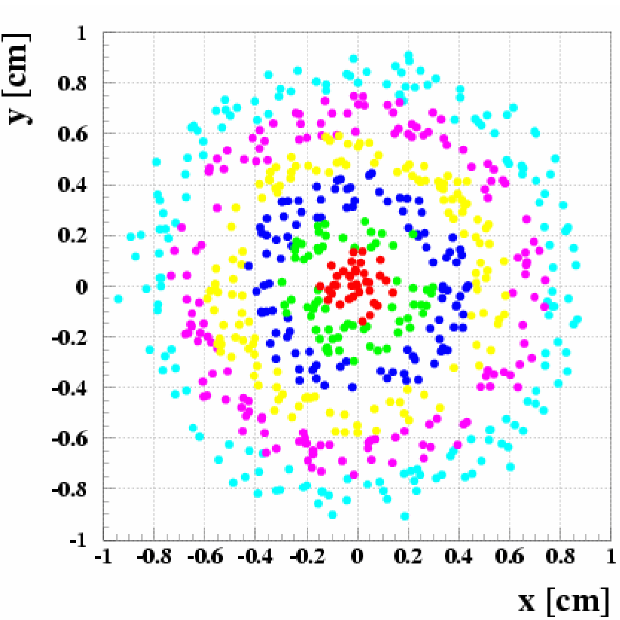

Hokuto Iijima

“ **C.A.S. 2005** **Intermediate Level Course on Accelerator Physics**”

Example of an optimized matching

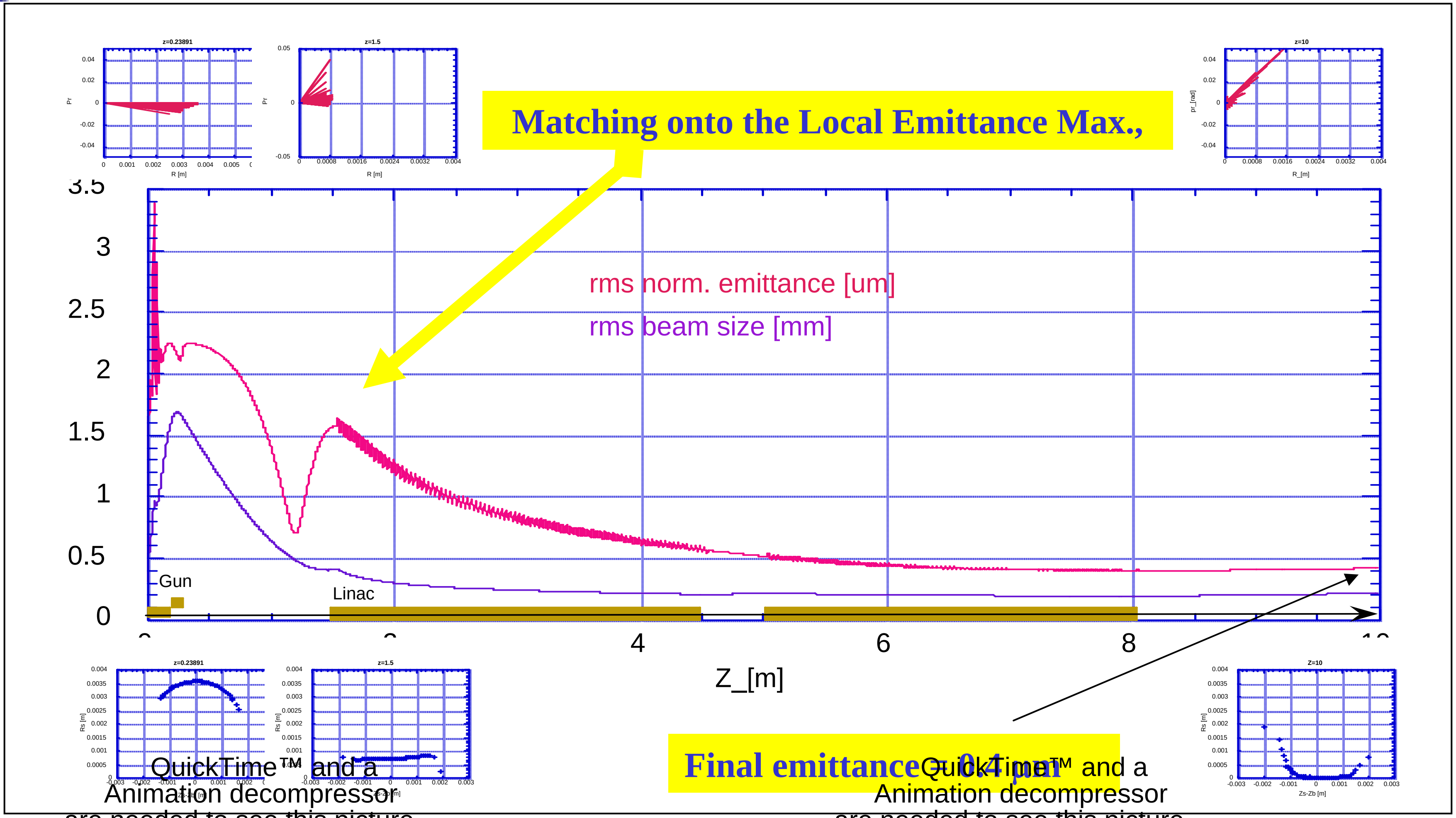

From Thermoionic Injectors to Laser-Driven RF Photo-Injectors : the Quest for Beam Brightness

Thermoionic Injectors operate in a quasi-steady state regime at low DC field amplitudes - the beam has to be manipulated by bunchers to get down to the ps time scale - this causes a severe emittance grow ⇒ **Integration of emission process into the bunching action of RF accelerating field**

⇒ ***RF Photo-Injectors Hera***

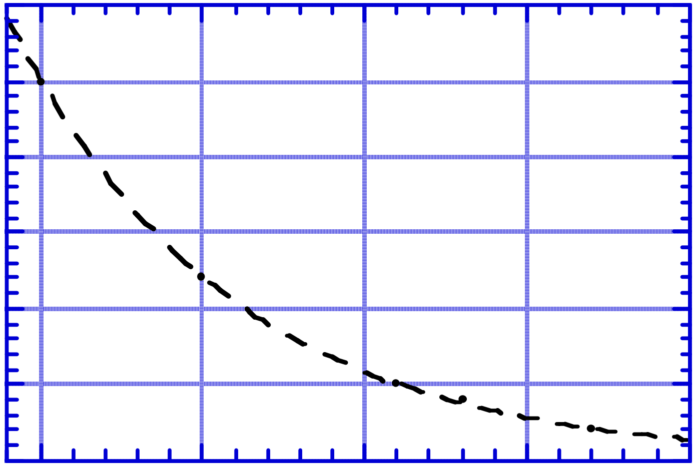

PhotoInjectors serve nowadays User Facilities, Advanced Accelerator Experiments, and...they make short wavelength SASE-FEL saturate!

BNL/SLAC/UCLA 1.6 cell S-Band RF GUN

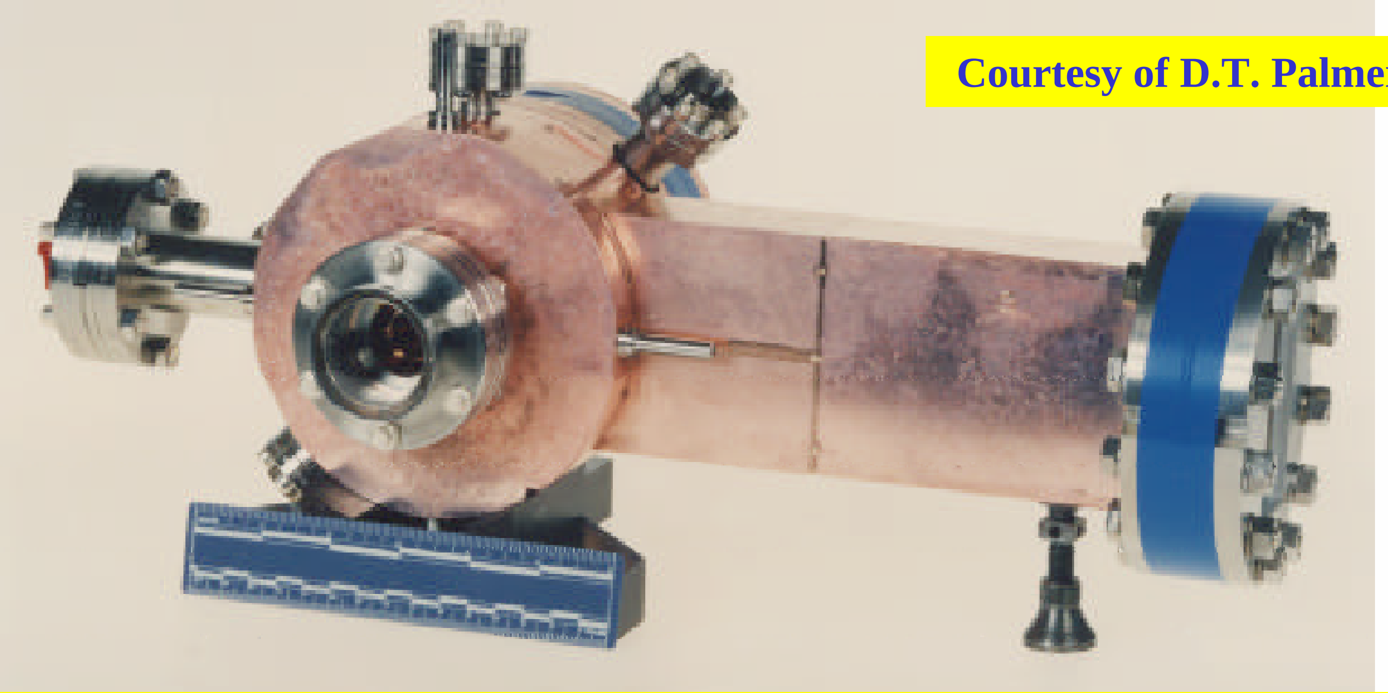

Courtesy of D.T. Palmer / SLAC

10 copies of this gun operated routinely around the world (USA, Japan) it holds the emittance record

Free Electron Lasers are based on Linear Accelerators
Beam quality needed to operate FEL's is crucially dependent on emittance produced by the injector (unlike circular accelerators)

The LCLS
(Linac Coherent Light Source)

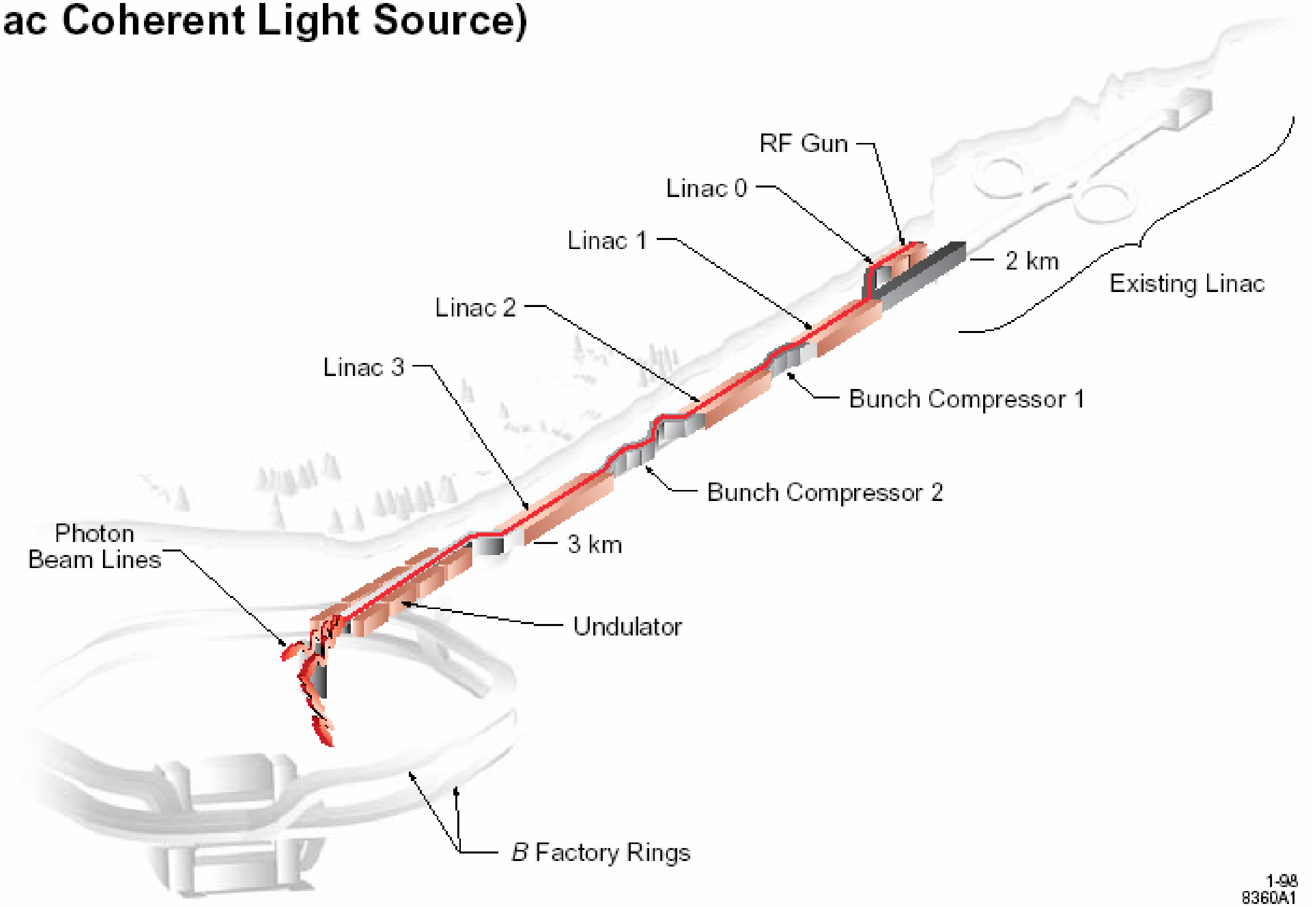

X-ray sources over the last 100 years: the story of a marriage between electron beams and X-rays

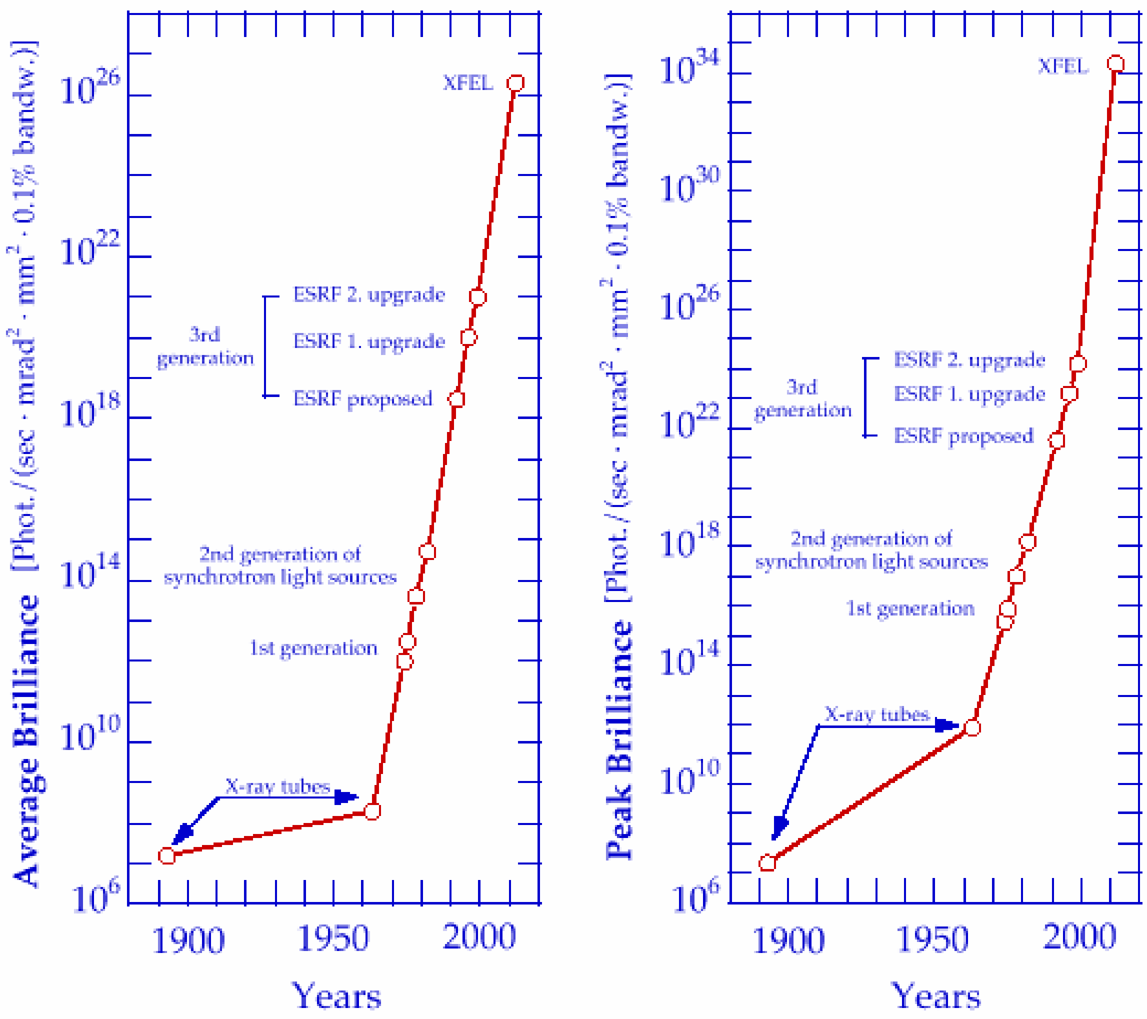

Suggested readings

J.S. Fraser et al., IEEE Trans. Nucl. Sci. NS-32 (1985), p.1791

R.L. Sheffield et al., Proc. 1988 Linear Accelerator Conf., Williamsburg, VA, Oct. 1988, CEBAF rep. 89-001 (1989), p.520

C. Travier, Particle Accelerators 36 (1991), p.33

K.J. Kim, NIM A275 (1989), p.201

B.E. Carlsten, IEEE Catalog no. 89CH2669-0 (1989) p.313

B.E. Carlsten et al., Proc. 1988 Linear Accelerator Conf., Williamsburg, VA, Oct. 1988, CEBAF rep. 89-001 (1989), p.365

L. Serafini, AIP Conf. Proc. 279 (1993), p.645 *and* L.Serafini, NIM A340 (1994), p.40

J.B.Rosenzweig and L.Serafini, Phys. Rev. E-**49** (1994), p.1599

S.C. Hartman and J.B.Rosenzweig, Phys. Rev. E-**47** (1993), p.2031

W.K.H. Panofsky and W.A. Wenzel, Rev. Sci. Instr. 27 (1956), p.967

More suggested readings

J.B. Rosenzweig and E. Colby, AIP CP 335 (1995), p.724

L.Serafini, Particle Accelerators 49 (1995), p.253

L. Serafini et al., NIM A387 (1997), p.305

L.Serafini and J.B.Rosenzweig, Phys. Rev. E-**55** (1997), p.7565

Proceedings of the ICFA 1999 Workshop on *The Physics of High Brightness Beams*, Los Angeles, 1999, Published on World Sci. ISBN 981-02-4422-3, June 2000

Proceedings of the ICFA 2002 Workshop on *Physics and Applications of High Brightness Beams*, Chia Laguna, Italy, 2002, in publication, see www.physics.ucla.edu/AABD

S. G. Anderson and J. B. Rosenzweig, PRSTAB **3** (2000), p. 094201-1

F. Zhou et al., PRSTAB **5** (2002), p.094203-1

More suggested readings

F. F. Chen, 1984, Introduction to Plasma physics, New York, Plenum.

J. L. Delcroix, 1980, Introduction to the theorie of ionized gases, New york, Wiley-Intersciences

I. G. Brown, 1989, The Physics and Technology of Ions sources, New york, Wiley-Intersciences

B. Wolf, 1995, Handbook of Ions Sources, London, CRC Press

C.E. Hill, Ion and Electron Sources, CERN, at www.cern.ch

Review of Scientific Instrument, Proceeding of International Conference On Ion Sources (since 1989)

H. Zhang, 1999, IonSources, Springer Verlag

Many thanks to Pascal Sortais (ISNG, Grenoble) for kindly providing various material on Ion Sources

X-Ray beam quality goes along with upgrade of electron beams

Since the invention of Crookes tubes (step! Roengten…)

DC 10^6 photons/s
in 1 $(mm{\cdot}mrad)^2$
0.1 % bandwidth

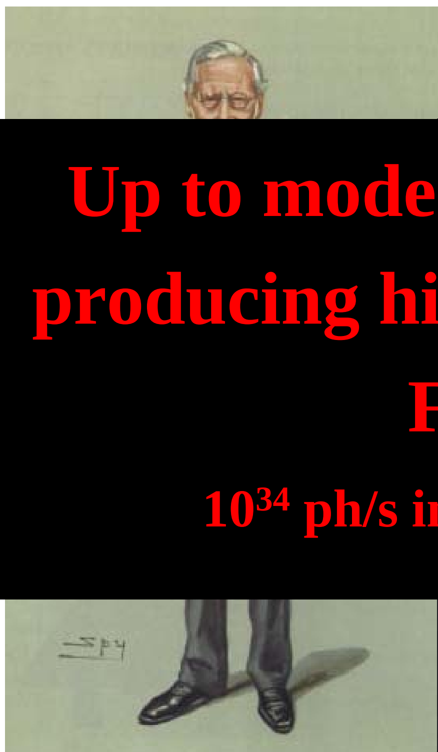

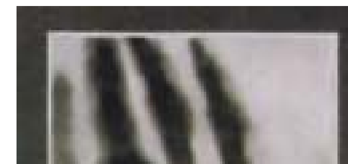

Up to modern (still under design) photo-LINACs producing high brightness electron beams to drive X-FELs (coherent X-ray beams)

10^{34} ph/s in 1 $(mm{\cdot}mrad)^2$ 0.1 % bandwidth 100 fs pulses

Laser layout

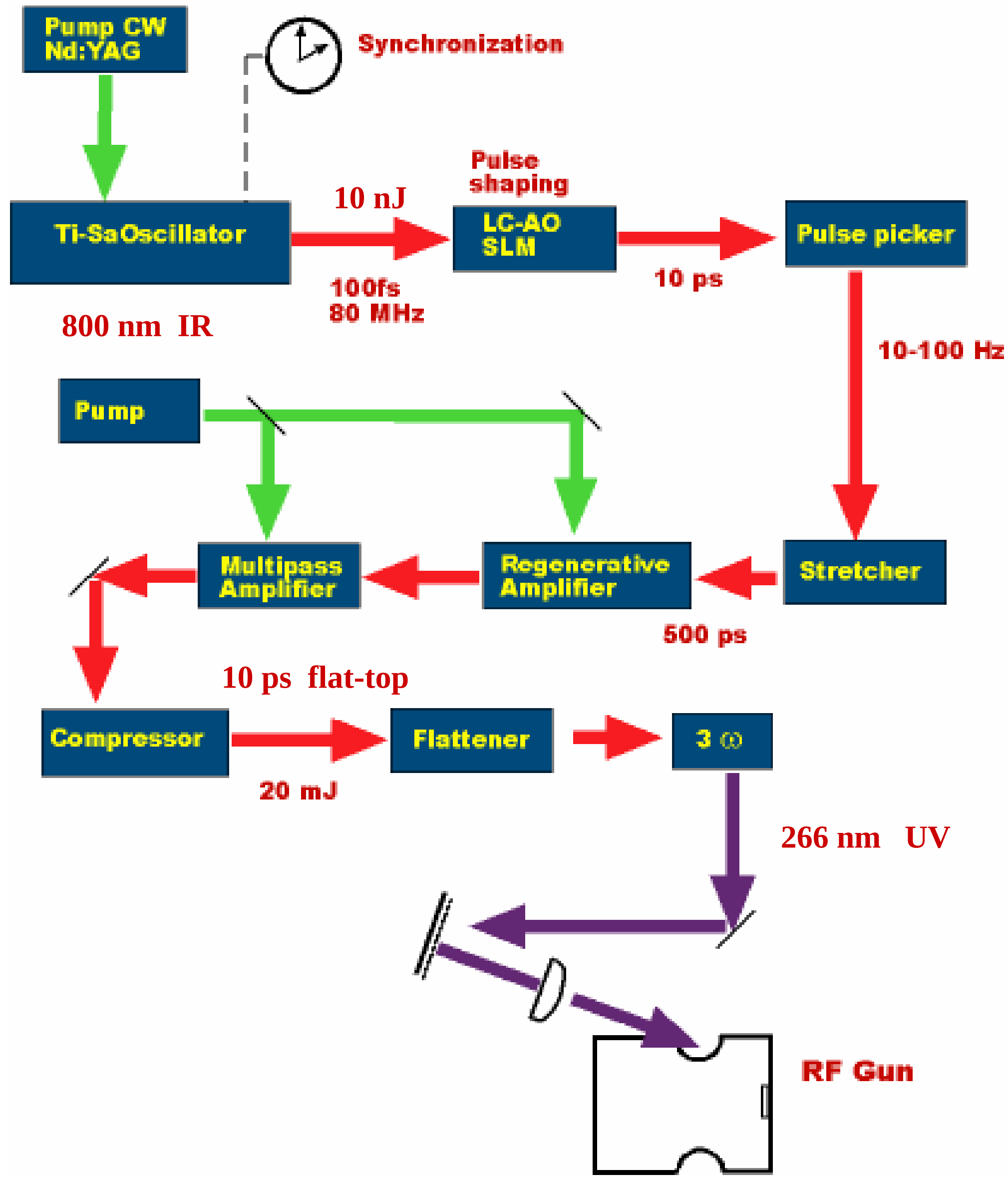

Major Issues in Laser System come from Stability Requirements

Phase jitter

Pointing Stability

Amplitude jitter

Transverse Brightness
RF Photo-Injector Achievements vs. Demands

TTF photo-inj. (achieved) **$6 \cdot 10^{12}$**
exit of linac (compr.) **$2 \cdot 10^{13}$**

ATF photo-inj. (achieved) **$5 \cdot 10^{13}$**
@ photocathode **$1.2 \cdot 10^{15}$**
Max. achievable without compr. $\varepsilon_{n\text{-}cath} = \varepsilon_{thermal}$

$$B_n \equiv \frac{2I}{\varepsilon_{nx}\varepsilon_{ny}} \left\lfloor \frac{A}{m^2 rad^2} \right\rfloor$$

I = bunch peak current

LCLS (requested @ 15 GeV) **$4 \cdot 10^{15}$**
$\varepsilon_{nx} = \varepsilon_{ny} = 1.5\ \mu m$

ESRF (storage ring) < **10^{14}**
$\varepsilon_{nx} = 20\ \mu m \quad \varepsilon_{ny} = 0.07\ \mu m$

Linac Coherent Light Source
@ SLAC
X-Ray Free Electron Laser

15 GeV e$^-$ beam using 1/3 of SLAC Linac

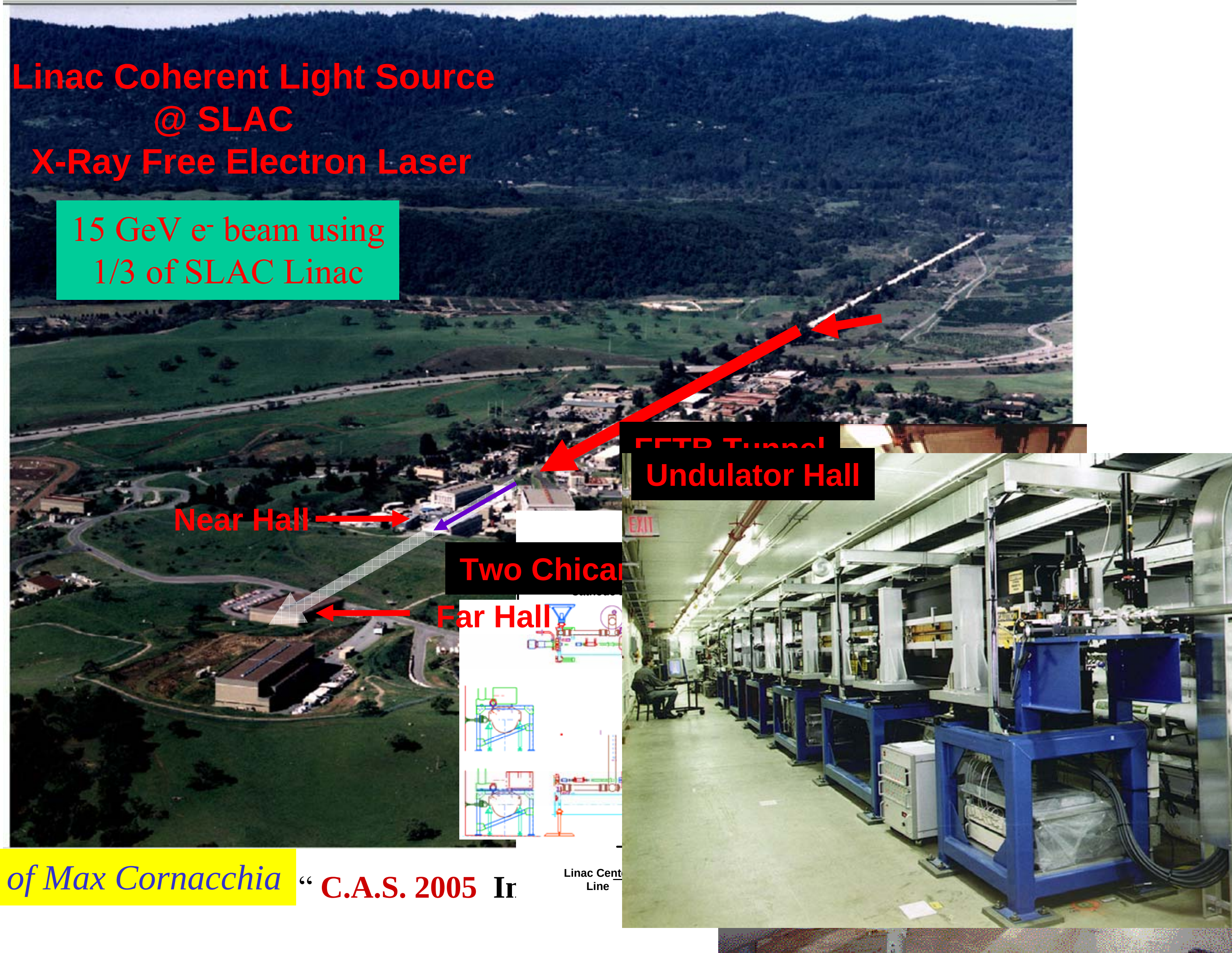

Courtesy of Max Cornacchia

“ C.A.S. 2005 Ir

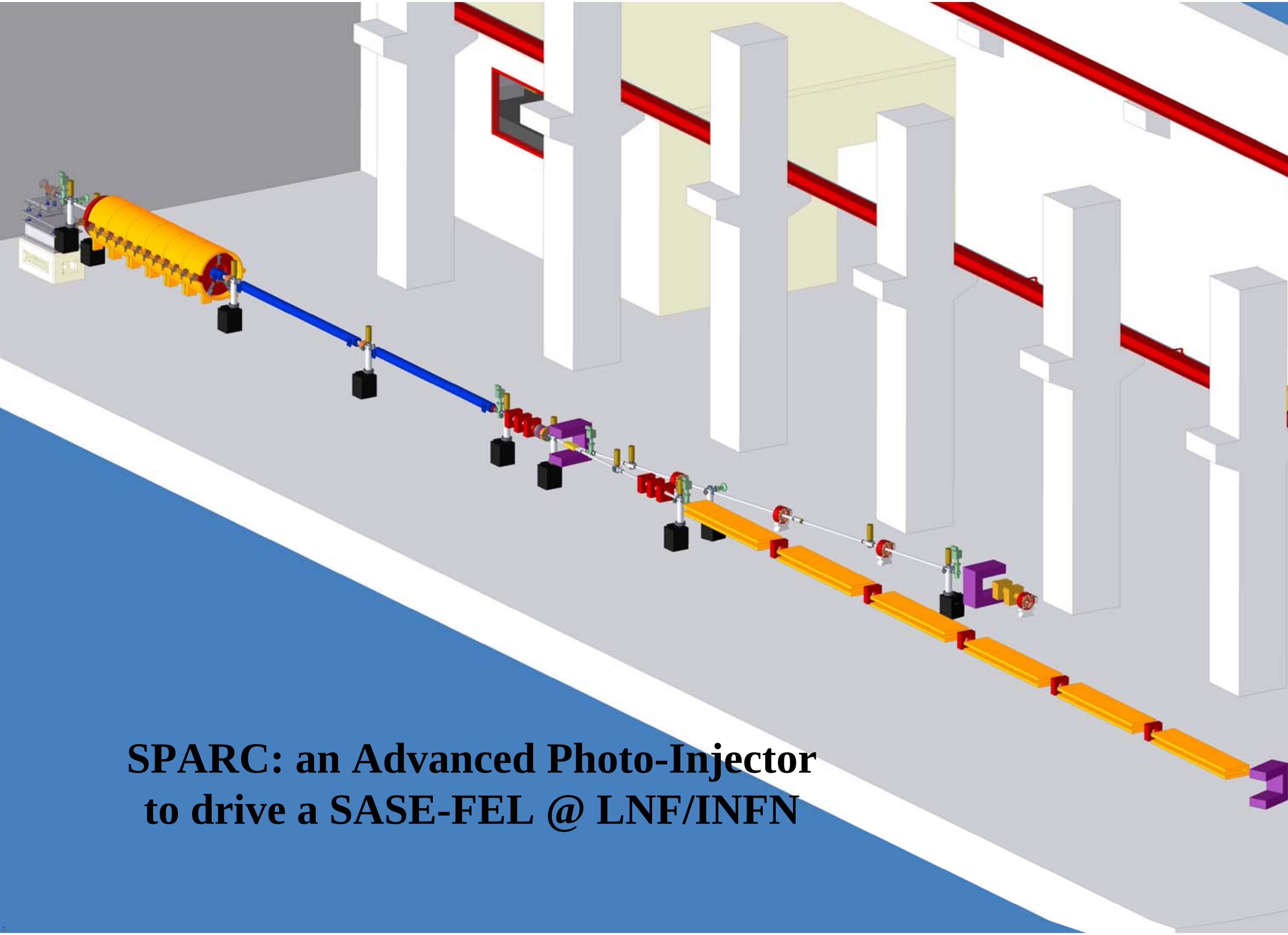

SPARC: an Advanced Photo-Injector to drive a SASE-FEL @ LNF/INFN